Title

Reactive transport of uranium in a groundwater bioreduction study: Insights from high-temporal resolution 238U/235U data

Authors

Shiel, AE
Johnson, TM
Lundstrom, CC
et al.

Publication Date

2016-08-01

DOI

10.1016/j.gca.2016.05.020

Peer reviewed

Reactive transport of uranium in a groundwater bioreduction study: Insights from high-temporal resolution $^{238}U/^{235}U$ data

Author links open overlay

panel A.E.Shiel[a] T.M.Johnson[b] C.C.Lundstrom[b] P.G.Laubach[b] P.E.Long[c] K.H.Williams[a]

Show more

https://doi.org/10.1016/j.gca.2016.05.020 Get rights and content

Abstract

We conducted a detailed investigation of U isotopes in conjunction with a broad geochemical investigation during field-scale biostimulation and desorption experiments. This investigation was carried out in the uranium-contaminated alluvial aquifer of the Rifle field research site. In this well-characterized setting, a more comprehensive understanding of U isotope geochemistry is possible. Our results indicate that U isotope fractionation is consistently observed across multiple experiments at the Rifle site. Microbially-mediated reduction is suggested to account for most or all of the observed fractionation as abiotic reduction has been demonstrated to impart much smaller, often near-zero, isotopic fractionation or isotopic fractionation in the opposite direction. Data from some time intervals are consistent with a simple model for transport and U(VI) reduction, where the fractionation factor (ε = +0.65‰ to +0.85‰) is consistent with experimental studies. However, during other time intervals the observed patterns in our data indicate the importance of other processes in governing U concentrations and $^{238}U/^{235}U$ ratios. For instance, we demonstrate that departures from Rayleigh behavior in groundwater systems arise from the presence of adsorbed species. We also show that isotope data are sensitive to the onset of oxidation after biostimulation ends, even in the case where reduction continues to remove contaminant uranium downstream. Our study and the described conceptual model support the use of $^{238}U/^{235}U$ ratios as a tool for evaluating the efficacy of biostimulation and potentially other remedial strategies employed at Rifle and other uranium-contaminated sites.

Keywords

Uranium isotopes
Isotope fractionation
Uranium reduction
MC-ICP-MS
Bioremediation

1. Introduction

Uranium (U) is the heaviest naturally occurring element on Earth. The two most abundant natural isotopes of U are ^{238}U and ^{235}U. These U isotopes decay to form stable ^{207}Pb (half-life of 4.468 billion years) and ^{206}Pb (half-life of 703.7 million years), respectively (Jaffey et al., 1971). Recent investigations (e.g., Stirling et al., 2007, Weyer et al., 2008) have revealed permil-level natural variations in the $^{238}U/^{235}U$ ratio. Mass-dependent fractionation of this magnitude is not expected for very heavy elements such as U. However, the observed isotopic fractionation is consistent with theoretical predictions (Bigeleisen, 1996, Schauble, 2007) of U isotopic fractionation by bonding differences due to nuclear size/shape among U isotopes during reduction–oxidation reactions. Nuclear volume fractionation results from differences in electron density at the nucleus for U(VI) compared to U(IV). Isotopes with a larger nucleus (i.e., ^{238}U) are more stable in sites with lower electron density at the nucleus; for U this is the U(IV) species, with two additional electrons. As a result, the larger isotope (^{238}U) is predicted to partition preferentially into the U(IV) species and the smaller isotope (^{235}U) into the U(VI) species at isotopic equilibrium. For U this partitioning during reduction–oxidation reactions is in opposition to mass-dependent fractionation. Theoretical predictions of kinetic isotope effects are not commonly done because the reaction mechanism, and in particular the transition states of the rate limiting steps must be known (Schauble, 2004).

Since the first studies reporting variable isotopic compositions for U, much effort has focused on improving our understanding of the mechanisms controlling U isotope fractionation. Laboratory studies have examined uranium isotope fractionation associated with biotic and abiotic processes. Equilibrium fractionation of 1.3–1.6‰ has been observed in laboratory experiments (Florence et al., 1975, Nomura et al., 1996, Fujii et al., 2006, Wang et al., 2015b). During laboratory microbial reduction, kinetic isotope fractionation has been shown to fractionate isotopes in the same direction as equilibrium fractionation, with the product isotopically heavy (Basu et al., 2014, Stirling et al., 2015, Stylo et al., 2015). In contrast, abiotic U(VI) reduction shows much smaller, often near-zero, isotopic fractionation (Rademacher et al., 2006, Stirling et al., 2007, Grimm, 2014, Stylo et al., 2015) or isotopic fractionation in the opposite direction (Stylo et al., 2015). Isotope shifts associated with U(VI) sorption consistent with mass dependent fractionation have also been observed (Stirling et al., 2007, Weyer et al., 2008, Brennecka et al., 2011, Holmden et al., 2015). This experimental work has been complimented by studies of natural environments where these processes occur.

Significant U isotope fractionation associated with redox processes has been observed in studies of, e.g., black shales (Stirling et al., 2007, Weyer et al., 2008), anoxic basin sediments (Weyer et al., 2008, Montoya-Pino et al., 2010, Andersen et al., 2014, Holmden et al., 2015, Noordmann et al., 2015, Hinojosa et al., 2016), and roll front U ore deposits (Bopp et al., 2009, Brennecka et al., 2010). Together these studies have demonstrated the potential of the $^{238}U/^{235}U$ ratio to serve as a geochemical tool capable of monitoring redox conditions in modern environments as well as reconstructing redox conditions in past environments.

One application in which U isotopes have shown potential is as redox monitors at current and former uranium mining and milling operations. A primary concern at these sites is uranium contamination of sediments and groundwater. In these systems, uranium is mobile in its oxidized state, U(VI), but largely immobile in its reduced state, U(IV) (Newsome et al., 2014). The use of native dissimilatory Fe-reducing microbes to catalyze the reduction of U(VI) in groundwater to insoluble U(IV) was first proposed as a remediation technique 25 years ago (Lovley et al., 1991) and numerous laboratory and field investigations of microbial reduction of soluble U(VI) are reviewed by Newsome et al. (2014). Microbes catalyze the transfer of electrons from a reduced species, such as acetate, to an oxidized species, such as Fe(III), in the process utilizing energy released by this redox reaction to carry out life functions. In the case of microbial reduction of Fe(III), or even S(VI), U(VI) may be concurrently reduced. Thus, groundwater amendment with acetate leads to the reduction of U(VI) to U(IV) by stimulating activity of native dissimilatory metal reducing microbes such as the Fe reducer *Geobacter* and sulfur reducing bacteria *Desulfobacter*.

This study focuses on the site of the Old Rifle processing plant in Rifle, CO, used to mill V–U ores from deposits in the Colorado Plateau area from 1924 to 1958. Before remedial action, a pile of mill tailings, waste produced from the processing of ores, ~10 m high, covering 4 km^2 existed at the Old Rifle site (DOE, 1999). In the early 1990s, the U.S. Department of Energy (DOE) took over management of the site and as a part of remedial actions removed the mill tailings, graded the site with fill material to produce a level base, and seeded with native range grasses. Despite these efforts, residual uranium contamination of the local aquifer remains. Persistence of this plume is attributed to the slow dissolution of naturally-occurring and contaminant U(IV) and the influx of U from natural upstream sources (Zachara et al., 2013). U.S. DOE-funded experiments have been conducted at the site as a part of the Rifle Integrated Field Research Challenge (IFRC) projects (Anderson et al., 2003, Williams et al., 2011, Long et al., 2015).

Uranium isotopes may be useful as a tool in monitoring remediation efforts by detecting and potentially quantifying reduction in the subsurface. Laboratory microbial reduction experiments have demonstrated that $^{238}U/^{235}U$ ratios vary systematically during microbial U(VI) reduction (Basu et al., 2014, Murphy et al., 2014, Stirling et al., 2015, Stylo et al., 2015), with isotopic shifts up to 5‰ documented in natural redox settings (Murphy et al., 2014). Further, Bopp et al. (2010) provided evidence for this isotopic shift (~1‰) with concentration in a field-scale biostimulation experiment at the Rifle site where U(VI) was reduced by acetate addition. In all these studies, the heavier isotope (^{238}U) was preferentially reduced to U(IV), leaving the remaining dissolved U(VI) pool with a relatively light isotopic composition (i.e., relatively low $^{238}U/^{235}U$ ratio).

Fractionation of $^{238}U/^{235}U$ ratios by sorption could potentially complicate the potential for U isotopes to track redox processes. However, existing studies suggest sorption is relatively unimportant in this setting. A small isotopic fractionation during U(VI) adsorption onto Mn-oxides was measured in laboratory experiments but the fractionation is much smaller than reduction and opposite in sense (Brennecka et al., 2011). Further, U isotopic fractionation induced by desorption and sorption has been shown not to cause significant shifts in $^{238}U/^{235}U$ ratios at the Rifle site (Shiel et al., 2013). The apparent discrepancy between the result of the laboratory and field experiments is suggested to result from differences in the U(VI) speciation (Shiel et al., 2013). In the laboratory experiment, there is a coordination change between the dissolved UO_2^{2+} and the U(VI) adsorbed onto Mn-oxides. In contrast, no change in the local U(VI) environment is expected during the adsorption of uranyl-carbonato and calcium-uranyl carbonato complexes to aquifer minerals.

To examine in detail the relationship between U(VI) reduction and $^{238}U/^{235}U$ ratios in a field setting, we present the results of two successive field biostimulation experiments performed at the Rifle site in 2010–11 and 2011–12. The 2010–11 experiment is well described in a recent publication (Long et al., 2015). The experimental plot is well instrumented and characterized, and dozens of samples were collected at each sampling point, daily in some cases, for each experiment to provide high temporal resolution of geochemical changes. Although a previous study (Bopp et al., 2010) presented $^{238}U/^{235}U$ ratio data for an earlier biostimulation experiment at Rifle, that data set was relatively sparse and so the authors were unable to extract the correct fractionation factor for U(VI) reduction. In the present study, we report $^{238}U/^{235}U$ ratio data at high temporal resolution and combine those results with other geochemical and physical measurements (most reported previously by Long et al. (2015)) that enable precise knowledge of relevant reaction and transport parameters of the system. Using

this large data set, we sought to (1) establish if U isotope fractionation is consistently observed across multiple experimental locations at the Rifle site; (2) determine the magnitude of isotopic fractionation for various conditions, including Fe(III)-reducing and sulfate-reducing phases, and at various times, such as the onset of reduction and the recovery phases after acetate injection ceased; (3) explore the fidelity with which $^{238}U/^{235}U$ ratio shifts track U(VI) reduction; (4) identify other processes, if they exist, which also cause $^{238}U/^{235}U$ ratio shifts or otherwise affect interpretation of the data; and (5) determine if re-oxidation of U sequestered as U(IV) during biostimulation can be detected as shifts in $^{238}U/^{235}U$ ratios within waters passing through the well array. We present a conceptual model for transport and U(VI) reduction in the Rifle aquifer, put forward hypotheses for observed patterns in the data, and discuss the implications for $^{238}U/^{235}U$ ratio studies at U remediation sites.

2. Analytical methods

2.1. Site description, experimental design and sample collection

Detailed descriptions of the site and its history are provided elsewhere (Anderson et al., 2003, DOE, 1999). In brief, the Rifle site is situated on a former uranium mill and processing facility located in Rifle, CO. All structures and the mill tailings piles and ponds have been removed leaving only residual contamination within the aquifer. Two apparently distinct uranium plumes exist, associated with the former locations of both the tailings pile and the ore storage area (DOE, 1999). The Rifle site is located on a floodplain of the Colorado River and is an unconfined aquifer composed of unconsolidated sands, silts, clays and gravel that overlie the relatively impermeable Wasatch formation at a depth of ~6.1 m (Williams et al., 2011). The aquifer materials are composed of Quaternary floodplain sediments dominated by quartz, with significant amounts of plagioclase and K-feldspar, smaller amounts of calcite, chlorite, kaolinite, smectite, illite and iron oxide minerals (primarily magnetite, goethite and aluminum-substituted goethite) (DOE, 1999).

Field experiments were conducted within an experimental test plot (Fig. 1) at the Rifle site. The experimental test plot (Plot C) consists of one row of background wells, two rows of injection wells and five rows of monitoring wells placed approximately perpendicular to groundwater flow, with a total footprint of ~13 m by ~12 m (Fig. 1). Wells are identified as either upstream or downstream of the injection wells as CU and CD, respectively. This plot is located within the contaminated aquifer underlying the site

of the former tailings pile. Linear groundwater flow velocity ranges from 0.4 to 0.6 m per day (DOE, 1999).

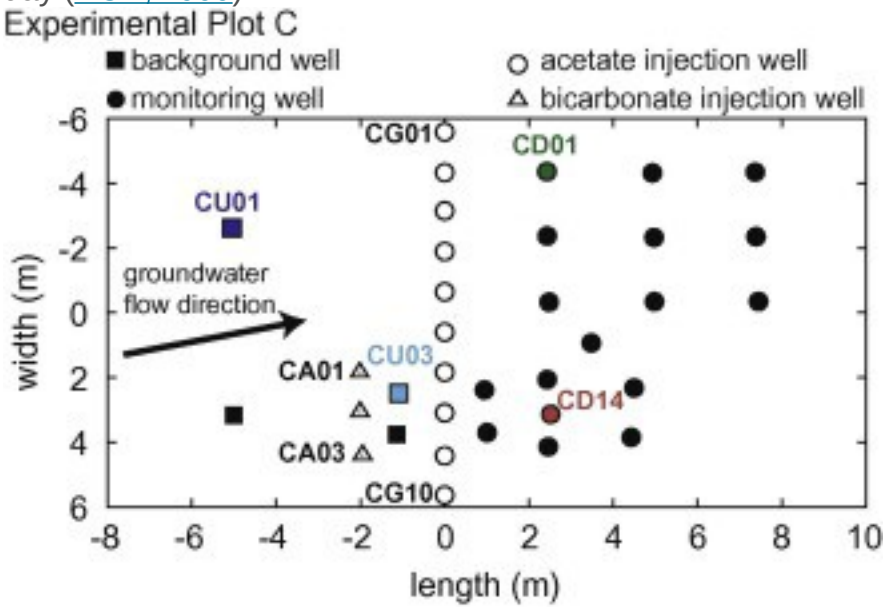

1. Download high-res image (138KB)
2. Download full-size image

Fig. 1. Map of experimental Plot C. Wells relevant to this study (i.e., background well CU01, injection wells CA01–CA03 and CG01–CG10, and monitoring wells CD01 and CD14) are identified. Groundwater flow is generally from left to right but is canted slightly such that flow lines from CU03 are unlikely to intersect CD14.

The impact of stimulated bioremediation on U concentrations and $^{238}U/^{235}U$ ratios was evaluated during consecutive field experiments ('Super 8' in 2010–11 and 'Best Western' in 2011–12) within experimental Plot C (Fig. 1). Summaries of injection parameters for both the 'Super 8' and 'Best Western' experiments are provided in Table 1. During both experiments "background" groundwater samples were collected from well CU01, located ca. 2 m upstream of the bicarbonate injection wells and 4 m upstream of acetate injection wells (Fig. 1). In addition, during the 'Super 8' experiment "background" groundwater samples were collected from well CU03, located ca. 1 m downstream of the bicarbonate injection wells and 1 m upstream of the acetate injection wells (Fig. 1). Results for CU03 have been published by Shiel et al. (2013).

Table 1. Injection parameters for the Super 8 and Best Western experiments.

Injection activity	Injection wells	Date	Duration (days)	Injectate concentration (mM)[a]	Injected volume (L)[a]	Isotope enrichment (‰)[a]
Super 8						
CH_3COONa and NaBr	CG01–CG10	Aug. 23–Sept. 7,	14	50 [CH_3COO^-]; 20 [Br^-]	2,200	

Injection activity	Injection wells	Date	Duration (days)	Injectate concentration (mM)[a]	Injected volume (L)[a]	Isotope enrichment (‰)[a]
		2010				
		Sept. 13–22, 2010	9	50 [CH_3COO^-]; 20 [Br^-]	1,500	
$NaHCO_3$ and D_2O	CA01–CA03	Aug. 16–27, 2010	11	50 [HCO_3^-]	6,000	380 (^2H)
		Aug. 29–Sept. 7, 2010	10	50 [HCO_3^-]	6,000	380 (^2H)
Best Western						
CH_3COONa and NaBr	CG01–CG05	Aug. 23–Nov. 3, 2011	72	150 [CH_3COO^-]; 20 [Br^-]	4,200	

a Concentrations are those in the injection tanks.

During the ‘Super 8’ experiment (August 2010), both bicarbonate and acetate were injected into the aquifer (Fig. 1). Acetate (3,700 L of 50 mM CH_3COONa) was injected into the aquifer over 23 days total (August 23–September 7 and September 13–22, with the 6-day period in between required to re-fill and re-mix the contents of the injection tank). This injectate was made from water from a nearby unimpacted well, doped with NaBr (to a concentration of 20 mM to serve as a conservative tracer) and sparged with N_2 to reduce dissolved oxygen content. The tank remained sealed under an N_2 headspace throughout the injection period. In addition, bicarbonate (12,000 L of 50 mM $NaHCO_3$) was injected into the aquifer over a 21-day period (August 16–27 and August 29–September 7, 2010, with the gap in between required to re-fill and re-mix the contents of the injection tank). This injectate was made from water from a nearby unimpacted well, enriched with D_2O (δ^2H = 500‰) as a conservative tracer to produce a bulk δ^2H of ∼380‰ and sparged daily with CO_2 to achieve and maintain a pH of ∼7. The ‘Super 8’ experiment allowed direct comparison between acetate injection alone and combined acetate and bicarbonate injections through sampling at monitoring wells CD01 and CD14, respectively (Fig. 1), because the bicarbonate injection doesn’t reach well CD01.

During the ‘Best Western’ experiment (August 2011), acetate (4,200 L of 150 mM CH_3COONa) was injected into the aquifer over a 72-day period (August 23–November 3, 2011). Like the ‘Super 8’ experiment, ‘Best Western’ involved adding NaBr and acetate to water from a nearby unimpacted well (sparged with N_2 to minimize oxygen

and sealed under N_2 headspace through the injection period). The purpose of 'Best Western' was to examine the impact of prolonged acetate injection through sampling of CD01 water (analogous to the shorter acetate only side of the 'Super 8' experiment). All groundwater samples (~20 mL) were collected from a depth of ~5 m, passed through 0.45 μm PTFE membrane filters and acidified to ~0.15 M with trace metal grade nitric acid(HNO_3). Groundwater samples were collected from background wells CU01 and CU03, and monitoring wells CD01 and CD14 (1) before the injections, (2) during the injections and (3) post-injection. The pH of CU01, CD01 and CD14 groundwater samples was monitored throughout the duration of the experiment. During the 'Super 8' experiment, the pH varied between 7.1 and 7.3 for CU01, 7.0 and 7.6 for CD01 and 7.1 and 7.4 for CD14. During the 'Best Western' experiment, the pH varied between 7.1 and 8.1 for CU01 and 6.8 and 8.0 for CD01.

2.2. Concentration determinations

Groundwater U concentrations were determined using inductively coupled plasma-mass spectrometry (ICP-MS) (Elan DRCII, Perkin Elmer, CA) at the Lawrence Berkeley National Laboratory. A subset of these samples was selected for U isotopic analysis.

2.3. Uranium double spike correction and sample preparation

Previous work demonstrates high precision U isotopic analysis is possible using a ^{233}U–^{236}U double spike (Stirling et al., 2005, Stirling et al., 2006, Stirling et al., 2007, Weyer et al., 2008, Bopp et al., 2009, Bopp et al., 2010). We added a spike with a $^{233}U/^{236}U$ ratio of ~0.45 (prepared in-house from ^{233}U and ^{236}U isotope spikes) to all samples prior to analytical separation of U. The double spike allowed for the correction of instrumental mass bias and any isotopic fractionation associated with the sample preparation. The reference material CRM 112A was spiked to give a $^{238}U/^{236}U$ ratio of ~30. Samples were spiked to give ratios of 18–34. Over-spiked ($^{238}U/^{236}U$ ratio of ~17) and under-spiked ($^{238}U/^{236}U$ ratio of ~56) reference materials were routinely run to demonstrate the measured U isotope ratiosare identical within uncertainty. Spikes were equilibrated with sample solution ~16 h before they were dried and then re-dissolved in 3 M HNO_3. U was purified by extraction chromatography using Eichrom UTEVA resin (~0.2 mL column; after Weyer et al. (2008)). After drying down the eluate, we spiked samples with ~20 μL 15 M HNO_3 and dried down, twice, to remove organic residues and then dissolved them in 0.30 M HNO_3 for MC-ICP-MS analysis.

2.4. Uranium isotopic measurements

Samples were analyzed for U isotopic composition using a Nu Plasma HR (Nu 039; Nu Instruments, UK) multi-collector inductively coupled plasma mass spectrometer (MC-ICP-MS) housed in the Department of Geology at the University of Illinois at Urbana-Champaign. A DSN-100 (Nu Instruments, UK) desolvator system was used for sample introduction. A modified sample–standard bracketing (SSB) measurement protocol was followed, where the standard was run after every three samples.

The measurement method was adapted from Bopp et al. (2009) and Bopp et al. (2010) and consisted of static measurements of masses 233–238 (isotopes of U). Sample ^{238}U was measured in a collector equipped with a 10^{10} Ω resistor for detection of large ^{238}U beams (allowing beam currents of up to 10^{-9} A), while the remaining isotope ion beams were measured in collectors with standard 10^{11} Ω resistors. An analysis comprised of 5 blocks of 10 × 8 s integrations. Samples were measured using a two zeros method, where zeros were measured at 0.5 amu above and below the measured mass for 30 s, and the average of those values was used to correct for background signal and tailing from neighboring peaks. This is especially important for correcting potential tailing of the ^{236}U peak onto that of ^{235}U. For all reference materials and samples, ^{238}U and ^{236}U signals were 1.5–8.0 × 10^{-10} A and 0.39–2.5 × 10^{-12} A, respectively.

Uranium isotopic compositions are reported relative to the U isotopic standard CRM 112-A (New Brunswick Laboratory, U.S. Department of Energy) in the standard delta notation:

$$‰\delta 238U = \left(\frac{238U}{235U}\right)_{sample} \left(\frac{238U}{235U}\right)_{standard} - 1 \times 1{,}000 (‰)$$

IRMM REIMEP 18-A and CRM 129-A (New Brunswick Laboratory, U.S. Department of Energy) were measured routinely. The running averages (±2S.D.) for IRMM REIMEP 18-A and CRM 129-A are −0.14 ± 0.08‰ (n = 24) and −1.70 ± 0.08‰ (n = 33), respectively. The running averages (±2S.D.) for CRM 112-A and IRMM REIMEP 18-A purified by extraction chromatography are 0.00 ± 0.06‰ (n = 21) and −0.14 ± 0.07‰ (n = 36), respectively. Twenty-three full procedural sample duplicates (Table 2) were analyzed and a modified root-mean-square calculation:

$$2\sigma = 2 \cdot \sum_{i=1}^{n} \frac{(ia - ib)^2}{2 \cdot n}$$

(Hyslop and White, 2009), where i_a and i_b refer to the two duplicate measurements of sample i, was used to determine the analytical uncertainty of the data, ±0.07‰ (95% confidence).

Table 2. Uranium concentration and isotopic results for background well CU01 and monitoring wells CD01 and CD14.

Date	Days[a]	U conc (μM)[b]	$\delta^{238}U$ (‰)[c]
Background well CU01			
7/31/2010	−16	0.77	0.11
8/18/2010	2	0.66	0.06
9/6/2010	21	0.62	
9/22/2010	37	0.62	0.08
10/11/2010	56	0.59	
10/21/2010	66	0.59	0.02
11/2/2010	78	0.58	
11/10/2010	86	0.59	0.06
12/9/2010	115	0.63	
1/20/2011	157	0.72	
2/24/2011	192	0.84	0.01
3/25/2011	221	0.82	0.01
4/26/2011	253	0.84	−0.03
5/20/2011	277	0.86	0.00
6/9/2011	297	0.83	
6/16/2011	304	0.78	
7/11/2011	329	0.76	
7/26/2011	344	0.73	0.05
8/9/2011	−14	0.64	0.03
8/9/2011 dup.	−14	0.64	0.06
Mean			0.04
8/23/2011	0	0.68	
8/31/2011	8	0.64	0.06
9/5/2011	13	0.64	0.00
9/5/2011 dup.	13	0.64	0.05
Mean			0.03
9/12/2011	20	0.64	
9/16/2011	24	0.63	
9/21/2011	29	0.62	0.03
9/26/2011	34	0.62	
9/30/2011	38	0.64	

Date	Days[a]	U conc (μM)[b]	$\delta^{238}U$ (‰)[c]
10/5/2011	43	0.63	
10/14/2011	52	0.62	0.04
10/19/2011	57	0.62	
10/24/2011	62	0.63	
10/31/2011	69	0.63	
11/4/2011	73	0.63	0.00
11/9/2011	78	0.64	
11/14/2011	83	0.65	
11/18/2011	87	0.64	
11/28/2011	97	0.64	
12/2/2011	101	0.66	−0.09
12/7/2011	106	0.67	
12/12/2011	111	0.67	
12/19/2011	118	0.64	
12/28/2011	127	0.64	
1/6/2012	136	0.63	0.00
1/13/2012	143	0.65	
1/20/2012	150	0.66	
1/27/2012	157	0.68	
2/8/2012	169	0.71	−0.05
2/21/2012	182	0.70	
3/8/2012	198	0.73	−0.01
3/22/2012	212	0.75	
4/5/2012	226	0.84	
4/10/2012	231	0.84	0.01
4/17/2012	238	0.84	
5/2/2012	253	0.89	
5/14/2012	265	0.88	0.02
5/22/2012	273	0.89	
5/29/2012	280	0.89	
6/6/2012	288	0.92	
6/13/2012	295	0.91	−0.01

Date	Days[a]	U conc (μM)[b]	δ^{238}U (‰)[c]
6/13/2012 dup.	295	0.91	0.02
Mean			0.00
6/21/2012	303	0.91	
6/28/2012	310	0.92	
7/5/2012	317	0.90	
7/12/2012	324	0.87	0.05
7/19/2012	331	0.84	
7/26/2012	338	0.84	
8/2/2012	345	0.84	0.04
8/15/2012	358	0.84	
Monitoring well CD01			
7/30/2010	−17	0.74	0.03
8/18/2010	2	0.70	
8/19/2010	3	0.69	−0.02
8/19/2010 dup.	3	0.69	0.03
Mean			0.01
8/24/2010	8	0.69	
8/25/2010	9	0.71	0.05
8/26/2010	10	0.68	
8/27/2010	11	0.74	0.02
8/28/2010	12	0.75	
8/30/2010	14	0.81	
8/31/2010	15	0.86	−0.07
8/31/2010 dup.	15	0.86	−0.11
Mean			−0.09
9/2/2010	17	0.81	−0.19
9/3/2010	18	0.69	−0.29
9/5/2010	20	0.47	−0.57
9/5/2010 dup.	20	0.47	−0.58
Mean			−0.57
9/7/2010	22	0.30	−0.83
9/9/2010	24	0.19	−0.93

Date	Days[a]	U conc (μM)[b]	$\delta^{238}U$ (‰)[c]
9/11/2010	26	0.14	−1.05
9/13/2010	28	0.09	−1.12
9/17/2010	32	0.06	
9/20/2010	35	0.05	−1.21
9/22/2010	37	0.05	
9/24/2010	39	0.04	
9/27/2010	42	0.03	
9/29/2010	44	0.04	−1.32
10/1/2010	46	0.05	−1.30
10/4/2010	49	0.07	
10/6/2010	51	0.10	−1.15
10/8/2010	53	0.11	−1.10
10/11/2010	56	0.12	
10/13/2010	58	0.15	−1.25
10/15/2010	60	0.16	−1.15
10/18/2010	63	0.18	
10/21/2010	66	0.22	−1.17
10/21/2010 dup.	66	0.22	−1.20
Mean			−1.18
10/25/2010	70	0.28	
10/28/2010	73	0.31	−1.00
11/1/2010	77	0.36	
11/4/2010	80	0.32	−0.92
11/4/2010 dup.	80	0.32	−0.90
Mean			−0.91
11/10/2010	86	0.46	
11/15/2010	91	0.52	−0.51
11/24/2010	100	0.58	
12/3/2010	109	0.61	
12/9/2010	115	0.69	
12/19/2010	125	0.72	−0.15
12/26/2010	132	0.75	

Date	Days[a]	U conc (μM)[b]	$\delta^{238}U$ (‰)[c]
1/8/2011	145	0.74	
1/20/2011	157	0.81	
1/28/2011	165	0.81	0.01
1/28/2011 dup.	165	0.81	−0.01
Mean			0.00
2/10/2011	178	0.86	−0.04
2/10/2011 dup.	178	0.86	−0.03
Mean			−0.03
2/24/2011	192	0.93	−0.01
2/24/2011 dup.	192	0.93	0.01
Mean			0.00
3/10/2011	206	1.00	0.04
3/25/2011	221	1.01	0.06
3/25/2011 dup.	221	1.01	0.02
Mean			0.04
4/11/2011	238	1.02	0.06
4/11/2011 dup.	238	1.02	−0.05
Mean			0.01
4/26/2011	253	1.02	0.03
5/11/2011	268	0.99	
5/20/2011	277	1.03	0.00
5/29/2011	286	1.01	
6/9/2011	297	0.99	
6/16/2011	304	0.90	0.01
6/30/2011	318	0.90	
7/11/2011	329	0.81	0.02
7/26/2011	344	0.82	0.01
8/9/2011	−14	0.77	0.03
8/23/2011	0	0.62	
8/29/2011	6	0.63	
8/29/2011	6	0.66	
8/30/2011	7	0.63	

Date	Days[a]	U conc (μM)[b]	$\delta^{238}U$ (‰)[c]
8/31/2011	8	0.60	−0.14
9/2/2011	10	0.40	−0.38
9/3/2011	11	0.40	
9/5/2011	13	0.24	−0.64
9/7/2011	15	0.15	−0.73
9/9/2011	17	0.10	−0.80
9/12/2011	20	0.07	−0.91
9/14/2011	22	0.07	−0.92
9/16/2011	24	0.06	−0.98
9/19/2011	27	0.05	
9/21/2011	29	0.05	−0.75
9/23/2011	31	0.04	
9/26/2011	34	0.05	
9/28/2011	36	0.05	−0.79
9/30/2011	38	0.05	
10/3/2011	41	0.09	−0.87
10/5/2011	43	0.08	
10/7/2011	45	0.09	
10/10/2011	48	0.11	−0.88
10/12/2011	50	0.09	
10/14/2011	52	0.10	−0.79
10/17/2011	55	0.08	
10/19/2011	57	0.08	
10/21/2011	59	0.08	
10/24/2011	62	0.08	
10/27/2011	65	0.07	
10/31/2011	69	0.07	
11/2/2011	71	0.07	
11/4/2011	73	0.07	
11/7/2011	76	0.08	
11/9/2011	78	0.09	
11/11/2011	80	0.09	

Date	Days[a]	U conc (μM)[b]	$\delta^{238}U$ (‰)[c]
11/14/2011	83	0.13	−0.99
11/16/2011	85	0.13	
11/18/2011	87	0.13	
11/23/2011	92	0.13	
11/28/2011	97	0.13	
11/30/2011	99	0.12	
12/2/2011	101	0.13	−1.01
12/5/2011	104	0.12	
12/7/2011	106	0.13	
12/9/2011	108	0.13	
12/12/2011	111	0.12	
12/15/2011	114	0.12	−1.18
12/19/2011	118	0.11	
12/22/2011	121	0.11	
12/28/2011	127	0.10	
1/3/2012	133	0.10	−1.06
1/6/2012	136	0.10	
1/10/2012	140	0.10	
1/13/2012	143	0.09	
1/16/2012	146	0.09	−1.22
1/20/2012	150	0.09	
1/24/2012	154	0.09	
1/27/2012	157	0.11	
2/1/2012	162	0.11	−1.52
2/8/2012	169	0.11	
2/14/2012	175	0.12	−1.69
2/21/2012	182	0.14	
2/28/2012	189	0.16	
3/8/2012	198	0.19	−1.89
3/15/2012	205	0.24	
3/22/2012	212	0.24	
3/29/2012	219	0.28	−1.62

Date	Days[a]	U conc (μM)[b]	δ^{238}U (‰)[c]
4/5/2012	226	0.33	
4/10/2012	231	0.33	
4/17/2012	238	0.37	−1.36
5/2/2012	253	0.45	−1.27
5/14/2012	265	0.47	
5/22/2012	273	0.53	−1.07
5/29/2012	280	0.54	
6/6/2012	288	0.62	
6/13/2012	295	0.65	
6/21/2012	303	0.62	−0.80
6/28/2012	310	0.60	
7/5/2012	317	0.61	−0.71
7/12/2012	324	0.61	−0.78
7/19/2012	331	0.66	
7/26/2012	338	0.62	
8/2/2012	345	0.66	
8/15/2012	358	0.67	
Monitoring well CD14			
8/3/2010	−13	0.66	−0.04
8/17/2010	1	0.55	
8/20/2010	4	0.61	0.01
8/20/2010 dup.	4	0.61	0.06
Mean			0.03
8/21/2010	5	0.47	
8/22/2010	6	0.48	
8/23/2010	7	0.64	−0.08
8/24/2010	8	0.62	
8/25/2010	9	0.74	−0.05
8/26/2010	10	0.86	
8/27/2010	11	1.13	
8/28/2010	12	1.36	−0.12
8/30/2010	14	1.57	

Date	Days[a]	U conc (μM)[b]	$\delta^{238}U$ (‰)[c]
8/31/2010	15	1.92	
9/3/2010	18	1.74	−0.25
9/5/2010	20	1.52	−0.13
9/5/2010 dup.	20	1.52	−0.16
Mean			−0.15
9/7/2010	22	1.08	−0.59
9/9/2010	24	0.52	−0.89
9/9/2010 dup.	24	0.52	−0.98
Mean			−0.94
9/11/2010	26	0.42	−0.85
9/13/2010	28	0.32	−1.09
9/17/2010	32	0.23	
9/20/2010	35	0.22	−1.03
9/22/2010	37	0.11	−1.09
9/24/2010	39	0.15	
9/27/2010	42	0.11	−0.91
9/29/2010	44	0.07	
10/1/2010	46	0.08	−0.87
10/4/2010	49	0.07	
10/6/2010	51	0.07	
10/8/2010	53	0.06	
10/11/2010	56	0.07	
10/13/2010	58	0.06	
10/15/2010	60	0.06	−0.85
10/18/2010	63	0.07	−0.81
10/21/2010	66	0.07	
10/25/2010	70	0.07	−0.78
10/28/2010	73	0.07	−0.92
11/1/2010	77	0.07	
11/4/2010	80	0.07	
11/10/2010	86	0.08	−0.86
11/15/2010	91	0.08	

Date	Days[a]	U conc (μM)[b]	$\delta^{238}U$ (‰)[c]
11/24/2010	100	0.09	−1.03
12/3/2010	109	0.11	
12/9/2010	115	0.12	−1.17
12/19/2010	125	0.16	
12/26/2010	132	0.19	−1.19
1/8/2011	145	0.22	−1.09
1/20/2011	157	0.29	−1.09
1/20/2011 dup.	157	0.29	−1.13
Mean			−1.11
1/28/2011	165	0.35	−0.99
1/28/2011 dup.	165	0.35	−0.98
Mean			−0.99
2/10/2011	178	0.37	−1.03
2/24/2011	192	0.53	−0.71
2/24/2011 dup.	192	0.53	−0.77
Mean			−0.74
3/10/2011	206	0.53	−0.65
3/25/2011	221	0.64	−0.43
3/25/2011 dup.	221	0.64	−0.52
Mean			−0.48
4/11/2011	238	0.64	−0.43
4/11/2011 dup.	238	0.64	−0.47
Mean			−0.45
4/26/2011	253	0.63	−0.36
5/11/2011	268	0.64	−0.39
5/29/2011	286	0.61	−0.43
6/9/2011	297	0.63	−0.33
6/16/2011	304	0.62	−0.34
6/30/2011	318	0.68	−0.29
7/11/2011	329	0.68	−0.30
7/11/2011 dup.	329	0.68	−0.25
Mean			−0.28

Date	Days[a]	U conc (μM)[b]	$\delta^{238}U$ (‰)[c]
7/26/2011	344	0.63	0.01
7/26/2011 dup.	344	0.63	0.09
Mean			0.05
8/9/2011	358	0.65	−0.19
8/9/2011 dup.	358	0.65	−0.25
Mean			−0.22
8/23/2011	372	0.66	−0.22
8/31/2011	380	0.60	−0.15

a

Days after first day of injection, 8/16/2010 and 8/23/2011 for years 1 and 2, respectively.

b

Concentrations provided by the Lawrence Berkeley National Laboratory group.

c

±0.07‰ (2 × the square root of the rms uncertainty for 23 full procedural duplicates).

The magnitude of isotopic fractionation, is described by the isotopic fractionation factor, α, where $\alpha = R_{product}/R_{reactant}$ and R is the $^{238}U/^{235}U$ ratio in the U(IV) product and U(VI) reactant pools. This quantity can be expressed in permil (‰) as ε, where $\varepsilon = 1000 \times (\alpha - 1)$.

3. Results

Changes in U concentration and $\delta^{238}U$ through time for upstream background well CU01, monitoring well CD01 (for acetate only injection) and monitoring well CD14 (acetate + bicarbonate injection) are shown in Fig. 2a–c and given in Table 2. Time is in days, with day zero being the first day of bicarbonate injection for the 2010–11 ‘Super 8’ experiment and acetate injection for the 2011–12 ‘Best Western’ experiment. Results for CU03 (effect of bicarbonate only) come from Shiel et al. (2013) and are shown in Fig. 2b. Fig. 2a and b compare the effects of acetate only and acetate and bicarbonate addition for the 2010–11 ‘Super 8’ experiment. Fig. 2c provides the extended acetate injection (2011–12 ‘Best Western’), which can be compared to the shorter acetate only injection of Fig. 2a. Concentrations of acetate, bromide (conservative tracer), and total inorganic carbon (TIC) are provided for the background and monitoring wells in Table A1.

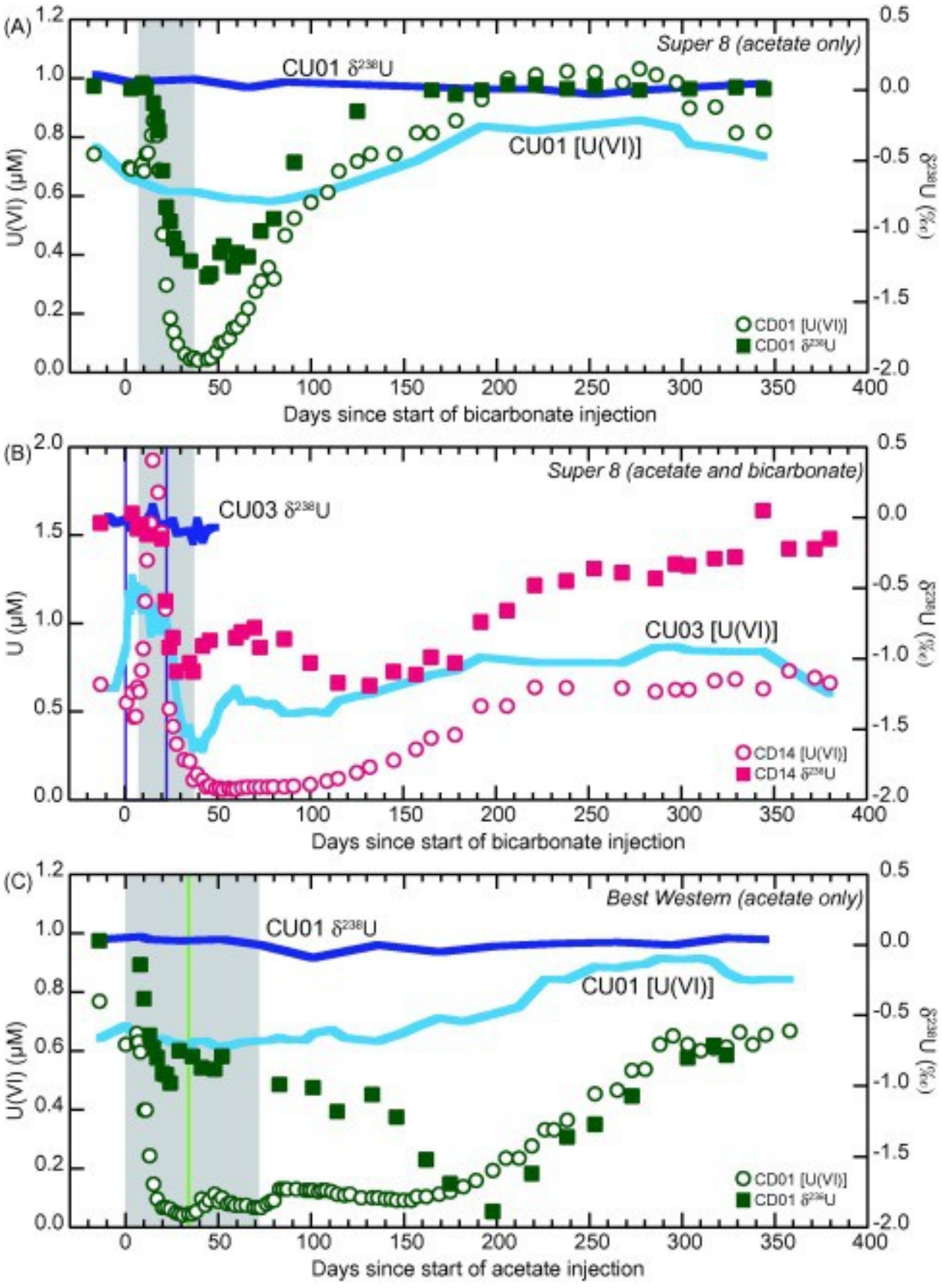
(A)
Super 8 (acetate only)
CU01 δ238U
CU01 [U(VI)]
U(VI) (μM)
δ238U (‰)
CD01 [U(VI)]
CD01 δ238U
Days since start of bicarbonate injection
(B)
Super 8 (acetate and bicarbonate)
CU03 δ238U
CU03 [U(VI)]
U (μM)
δ238U (‰)
CD14 [U(VI)]
CD14 δ238U
Days since start of bicarbonate injection
(C)
Best Western (acetate only)
CU01 δ238U
CU01 [U(VI)]
U(VI) (μM)
δ238U (‰)
CD01 [U(VI)]
CD01 δ238U
Days since start of acetate injection

1. Download high-res image (685KB)
2. Download full-size image

Fig. 2. Temporal trends of U concentration (circles) and $\delta^{238}U$ (squares) for groundwaters from the ‘Super 8’ experiment (A, B) and the ‘Best Western’ experiment (C). (A) shows results from the eastern half of the experimental plot of ‘Super 8’ where only acetate is injected; (B) shows the western half of the experimental plot which combined bicarbonate injection with acetate injection. Vertical gray bands show timing of acetate injection while blue lines denote bicarbonate injection timing. U concentration (light blue line) and $\delta^{238}U$ (dark blue line) are shown for input groundwaters from background wells CU01 (A) and CU03 (B). [U] and $\delta^{238}U$ data from monitoring well CD01 (green) (A) show good correspondence, consistent with isotopic changes reflecting chemical reduction of U(VI). In (B), while data from CD14 (red) also indicate correspondence, concentrations are strongly affected by desorption and readsorption thus complicating the [U]–$\delta^{238}U$ relationship. (C) Results for the extended acetate injection experiment ‘Best Western’ (year 2). U concentration (light blue line) and $\delta^{238}U$ (dark blue line) are shown for input groundwaters from background well CU01. The vertical green line identifies the shift from primarily iron reduction to sulfate reduction (Long et al., 2015). Data show the extended period of low concentration U and two-stage drop in $\delta^{238}U$. (For interpretation of the references to colour in this figure legend, the reader is referred to the web version of this article.)

3.1. Background geochemical conditions

3.1.1. Background well (CU01)

Because of its location upstream of the injection galleries, CU01 provides information about the initial composition of water moving into Plot C. The U concentration of groundwater from well CU01 varied between 0.58 and 0.86 μM during the first year (day −27 to 344), and between 0.62 and 0.92 μM in the second year (day −14 to 358; Table 2 and Fig. 2a). This variation in concentration is attributed to seasonal changes in groundwater elevation associated with increased runoff from snowmelt during the spring and early summer. Elevated groundwater leads to the release of adsorbed U(VI) during the spring/early summer, with the highest concentrations occurring in the late spring (June) and the lowest in the late fall (October).

The $\delta^{238}U$ values of groundwater samples from background well CU01 varied from −0.03‰ to 0.11‰ and −0.09‰ to 0.06‰ during the first and second years, respectively (Table 2 and Fig. 2a). The two-year combined data set yielded a 2S.D. of ±0.08‰, which is very close to the analytical uncertainty. Therefore, despite significant seasonal variation in groundwater U concentration, no significant variations in $\delta^{238}U$ occur,

indicating that all downstream variations in $\delta^{238}U$ reflect processes within the experimental plot.

3.1.2. Background well (CU03)

This well is located downstream of the bicarbonate injection gallery and upstream of the acetate injection gallery, on the western side of plot C. CU03 thus provides information about the initial composition of water moving into the reducing zone created by the acetate injection in the combined bicarbonate-acetate experiment of 'Super 8' (Fig. 2b and Table A1). Groundwater amendment with bicarbonate leads to the desorption of U(VI) from mineral surfaces by increasing the relative abundance of highly stable calcium-uranyl carbonato species (Stewart et al., 2010, Fox et al., 2012) thus increasing groundwater U concentrations.

CU03 variations during the 'Super 8' experiment (Fig. 2b) thus provide information about the compositions of waters entering the acetate treatment zone. Prior to the start of the bicarbonate injection, the U(VI) concentration of groundwater from well CU03 was ~0.63 μM. As bicarbonate increased during the injection phase (day 0–22; Fig. 2b), U concentration increased (Fig. 2b) reflecting U(VI) desorption from aquifer sediments. The U(VI) concentration doubled to a maximum concentration of ~1.26 μM (day 4; Fig. 2b). After day 8, the U concentration decreased, presumably reflecting U(VI) depletion from mineral surfaces (Fig. 2b). As bicarbonate was flushed out of the experimental plot post-injection (after day 22), the U concentration decreased further (Fig. 2b). Fifteen days after the injection ceased, U concentrations had decreased to a minimum concentration of 0.29 μM (day 42), which is less than half that observed in pre-injection groundwater (Fig. 2b). Assuming this groundwater advected into the experimental plot with a U(VI) concentration of approximately 0.63 μM (similar to CU01 at this time), the water must have lost U(VI). We attribute this loss to adsorption of U(VI) back onto sorption sites opened up by the bicarbonate flush (Long et al., 2015). As these newly available sites became repopulated, U concentrations increased rapidly (days 47–50) ultimately returning to background values (0.49–0.87 μM) from day 50 to 380 (Fig. 2b).

The $\delta^{238}U$ values of groundwater samples from background well CU03 varied from −0.19‰ to 0.08‰ during and immediately following the bicarbonate injection (day −9 to 49; Fig. 2b) (Shiel et al., 2013). The data set yielded a 2S.D. of ±0.11‰, which is identical to the reported analytical uncertainty (±0.11‰) (Shiel et al., 2013). Thus despite a doubling of concentration due to desorption, no measurable changes

in $^{238}U/^{235}U$ ratios were observed through day 50; we assume that like CU01, no changes in $^{238}U/^{235}U$ ratios occurred in CU03 groundwater throughout the rest of the experiment.

3.2. Short duration acetate injection (2010–2011 'Super 8') experiment

3.2.1. Eastern side of plot: acetate injection only

Monitoring well CD01 was impacted by the acetate injection (day 7–37; Table 1) but not by the bicarbonate imposed on the western half of the experimental plot (Fig. 1). Prior to the start of the injection, the U concentration was ~0.68 μM (Fig. 2a). During the initial phase of the injection, acetate and the co-injected bromide tracer increased in the well and the U concentration decreased rapidly (Fig. 2a and Table A1). U concentrations decreased smoothly over 35 days to a minimum of 0.03 μM, about 5% of the concentration in upstream well CU01 at that time (Fig. 2a). The presence of elevated acetate and bromide in the vicinity of CD01 confirms the presence of the injectate throughout the period from day 9 to 49 (Table A1; Long et al., 2015). Injection ceased on day 37, and as acetate concentrations dropped in the experimental plot, U concentrations increased concurrently (Fig. 2a) returning to background levels approximately 100 days after the injection ceased.

Total inorganic carbon (TIC; predominantly HCO_3^-) concentration is important, as it influences U(VI) speciation and adsorption (see Section 4). Two peaks in TIC concentration occurred, with maximum concentrations of 12.7 and 12.2 mM found on days 12 and 44, respectively (Table A1; Long et al., 2015). These concentrations are about 45% larger than those found in background well CU01 during the 2010–11 experiment. We attribute this difference to two processes. First, bicarbonate was produced as a result of acetate oxidation accompanying microbial respiration. Second, an unintended, minor incursion of injected bicarbonate, which targeted the western side of the plot, crossed over into the eastern side near well CD01 (evidenced by the presence of the D_2O tracer injected with the bicarbonate). This occurred because of cross-well mixing among the acetate injection wells, a process designed to generate uniform acetate concentrations across the injection gallery (day 11). This incursion led to a small U concentration increase to ~0.86 μM from day 11 to day 15, reflecting U(VI) desorption due to a relatively small increase in bicarbonate.

3.2.2. CD01 groundwater $\delta^{238}U$ values

Concomitant with U concentration decreasing upon the start of acetate injection, the $\delta^{238}U$ at CD01 decreased strongly (Table 2 and Fig. 2a). Pre-injection samples exhibited $\delta^{238}U$ values of ~0.0‰, equal to those of upstream well CU01. $\delta^{238}U$ values then decreased smoothly to a minimum of −1.32‰ (Fig. 2a), coinciding with the minima in U

concentration that occurred at termination of acetate injection. As acetate was flushed out of the plot and reduction slowed, both $\delta^{238}U$ and dissolved U concentrations increased in parallel. Concentrations attained values equal to those of background (CU01) about 90 days after acetate injection ceased, then maintained values slightly greater than those of CU01 after that time. $\delta^{238}U$ returned to initial values (0.0‰, identical to CU01) about 120 days after injection ceased and remained at 0.0‰ for the remainder of the monitoring period.

3.2.3. Western side of plot: combined bicarbonate and acetate injection

Monitoring well CD14 was impacted by both the bicarbonate injection (day 0–22) and the acetate injection (day 7–37) (Table 1). Prior to the start of the injections, the U concentration of groundwater from well CD14 was ~0.66 μM (Fig. 2b). During the initial phase of only bicarbonate injection, measured δD and TIC increased (Table A1; Long et al., 2015). Like CU03, U concomitantly increased (Fig. 2b) due to bicarbonate induced desorption. However, the U concentration nearly tripled (~1.9 μM) (Fig. 2b), reflecting the greater contributing volume of sediments, and hence inventory of sorbed U(VI), as compared to the CU03 flowpath. During this pre-acetate injection time, U concentration at CD14 was closely related to the TIC concentration, conforming approximately to the relationship [U] = 17.6 × TIC (Long et al., 2015). However, increases in U concentration halted when acetate levels began to rise, despite TIC continuing to rise (Table A1).
A similar increase in the U concentration occurred in CU03 (Fig. 2b), the upstream well impacted by the bicarbonate injection but not the acetate injection (Shiel et al., 2013). The increase was smaller in CU03 because the bicarbonate-rich water had traveled a smaller distance at that point and thus desorption gains were smaller. Accordingly, although CU03 provides information about sorption, we note that it is not an accurate indicator of the U concentration entering the western zone of the experimental plot, near well CD14 due to the placement of wells relative to groundwater flow direction (Fig. 1).
Injection of acetate and bromide began on day 7 (Fig. 2b) with their arrival at CD14 on day 10 (Table A1). Maximum acetate concentrations were about one quarter of those in well CD01. Once acetate concentration exceeded 1 mM (Long et al., 2015), U concentration decreased rapidly, falling over a period of 35 days to a minimum of 0.06 μM. This minimum was reached a few days after acetate injection terminated. Notably, U concentration then remained low for about 30 days before increasing gradually (Fig. 2b). This contrasts with U concentration behavior in monitoring well CD01 which rebounded within ~12 days. Some of the lag seen in CD14, may be due to adsorption losses as open sorption sites were repopulated. However, the U

concentration recovery at CU03 occurred in a few days, whereas U concentration in CD14 remained low for up to 50 days.
Recovery to a stable U concentration occurred ~180 days after the injection ceased, although it remained ~25% lower than in the background well (CU01) until approximately day 350 (Fig. 2b). Thus, the recovery time for the combined bicarbonate and acetate treatment (CD14) is much longer than that observed for the acetate injection alone (CD01; Fig. 2b).

3.2.4. CD14 groundwater $\delta^{238}U$ values

Pre-injection groundwater samples exhibited a $\delta^{238}U$ value of −0.04‰ (Fig. 2b) equal to those from background wells CU01 and CU03. No changes were observed in early samples, prior to the onset of U(VI) reduction, despite U concentration increasing due to bicarbonate-induced desorption. $\delta^{238}U$ values in well CU03 (Fig. 2b) impacted by bicarbonate injection (but not acetate injection) similarly showed no change in $\delta^{238}U$ in response to desorption (Shiel et al., 2013).
The $\delta^{238}U$ of CD14 waters decreased to a minimum of −1.09‰, as U concentration decreased in response to the acetate-induced U(VI) reduction (Fig. 2b), following the same behavior observed at CD01 (impacted by acetate alone). Whereas both U concentration and $\delta^{238}U$ increased in sync upon acetate termination in CD01, both U concentration and $\delta^{238}U$ behaved entirely differently at CD14. Upon acetate termination, $\delta^{238}U$ of CD14 rebounded to −0.78‰ on day 70 (Fig. 2b) followed by decreasing again to −1 on day 120. This second low corresponds to a time when the U concentration is beginning to increase again after the 50 days of sustained low U concentrations. Indeed, $\delta^{238}U$ values recovered even more slowly than U concentrations, not clearly recovering to background levels as of day 380, the end of the experiment (Fig. 2b).

3.3. Long duration acetate injection (2011–2012 ‘Best Western’) experiment

3.3.1. Monitoring well (CD01)

Monitoring well CD01 was subjected to a second, prolonged (72 day) acetate injection in year 2 (day 0–72; Table 1). Acetate levels were intentionally higher, with the maximum concentration in CD01 approximately 3 times that observed during year 1 (Table 1). Prior to the start of the injection, the U concentration of groundwater from well CD01 was ~0.63 μM (Fig. 2c). During the acetate injection, U concentrations fell to a minimum of 0.04 μM (day 31), which is ~7% of the concentration observed in groundwater from background well CU01 at the same time (Fig. 2c). A small increase in the U concentration accompanies the onset of sulfate reduction, as evidenced by a

dramatic drop in sulfate levels and a concurrent increase in S^{-2} levels around day 34 (Long et al., 2015).

Once acetate injection ended, sulfate levels increased (and S^{-2} levels decreased) slowly, returning to background levels ~100 days after the injection ends (Long et al., 2015). U levels increased slightly to ~0.08–0.13 μM, and then remained at this low level for ~100 days, before gradually increasing. U levels stabilized from day 288 to 358 (0.60–0.67 μM), remaining lower than those of upstream water (~0.84 μM). At the end of the experiment (day 358), the U concentration and isotopic data indicate that reduction was still occurring.

A large peak in the total inorganic carbon (TIC) is observed with a maximum concentration of 26.5 mM occurring on day 73 (Table A1). This concentration is more than double the size of the peak observed in year one (12.2 mM; Table A1). The much higher TIC levels during 'Best Western' reflect increased microbial bicarbonate production due to the relatively high acetate concentrations, combined with the occurrence of sulfate reduction, which produces more TIC than Fe reduction per the stoichiometry of the reactions (Langmuir, 1997).

3.3.2. CD01 groundwater $\delta^{238}U$ values

The $\delta^{238}U$ value in CD01 waters prior to injection is 0.03 ± 0.07‰. As acetate was injected into the plot, $\delta^{238}U$ decreased along with dissolved U concentration (Fig. 2c), reaching an initial minimum of –0.98‰ on day 24 (Fig. 2c). A small rebound in $\delta^{238}U$ corresponds (Fig. 2c) to the shift from Fe reduction to sulfate reduction in the plot (Long et al., 2015).

For ~50 days post-injection (day 83–133), the U concentration and $\delta^{238}U$ remained relatively constant at ~0.08–0.13 μM and ~−1.00‰. During the period from day 133 to 195, $\delta^{238}U$ strongly decreased from ~−1.00‰ to −1.89‰. U concentrations steadily increased from 0.1 μM at day 150 to 0.65 μM at day 290. The $\delta^{238}U$ began to increase on about day 195 (>120 days post-injection) and remained much less than initial input at the end of the experiment with a value of ~−0.80‰.

4. Discussion

4.1. Processes governing U concentration and $\delta^{238}U$ in CD01 and CD14

The observed changes in $\delta^{238}U$ and U concentration as groundwater passed from the upstream area, sampled by wells CU01 and CU03, to CD01 and CD14 impacted by the experimental manipulations, resulted from various reaction and transport processes in the aquifer. Given the known configuration and manipulation of the experimental plot and the geochemical properties of U, we identified five processes that were involved: (1)

transport of dissolved U(VI) with groundwater flow; (2) U(VI) reduction and the precipitation of the product U(IV) from solution; (3) adsorption and desorption in response to changes in dissolved U concentration and/or speciation; (4) “memory” of past conditions cause by exchange of dissolved U(VI) between faster flowing domains of the aquifer and lower permeability domains that are not rapidly flushed; and (5) oxidation and remobilization of U(IV) as reducing conditions wane and oxidants re-enter U(IV)-bearing zones. As we argue below, the patterns observed in the data were created by all of these processes.

4.1.1. Transport, adsorption, and desorption

Though upstream background wells CU01 and CU03 are not perfect indicators of the U concentration in the inflowing waters, they provide a reasonable approximation of the U concentration and $\delta^{238}U$ of water that is the inflow to the reducing zone. While the groundwater flow direction is generally from north to south (left to right in Fig. 1) in the experimental plot, the flow direction changes somewhat over time in response to variation in the level of the Colorado River and other seasonal hydrologic changes. While background wells are not necessarily on the same flow path as the observed CD01 and CD14 wells, total travel is only a few days and the upstream wells in most cases do not change rapidly.

The HCO_3^- injection in the western side of the plot caused the inflow U concentration at the upstream edge of the reducing zone to depart from that measured in the upstream well CU01. The injection caused a strong release of adsorbed U(VI) into solution; this roughly doubled the U concentration in CU03 (Fig. 2b), located about 1 m downstream of the HCO_3^-injection wells. The U concentration peaked quickly and began to decrease as the adsorbed pool became depleted. Immediately after the bicarbonate injections ceased, U concentration decreased quickly to about half the background level and eventually recovered 25 days after the injection ceased. The inflow at the upstream edge of the reducing zone, about 2 m downstream of the HCO_3^- injection wells, must have responded similarly, but with a greater amplitude of change, as the HCO_3^- acted on about twice as much aquifer material. This is reflected in well CD14’s U concentration, which roughly tripled before acetate-induced bioreduction caused it to decrease (Fig. 2b). Because of the strong sorption-related effects, CU03 is not a precise indicator of inflow concentration during the bicarbonate injection and its aftermath, making it difficult to precisely determine the effects of U(VI) reduction on concentrations measured in CD14, as we discuss below.

The eastern side of the plot, as represented by well CD01, was also mildly impacted by desorption and re-sorption, because some of the bicarbonate injected in the western side was moved eastward by cross-well mixing in the acetate injection gallery. This is exhibited in the brief U concentration increase in well CD01 just before the onset of reduction (Fig. 2a).

4.1.2. Rayleigh distillation: a simple model for transport and U(VI) reduction

As groundwater passes the acetate injection gallery, U concentration decreases reflecting precipitation of U(IV) and causing an isotopic fractionation (Anderson et al., 2003, Holmes et al., 2007, Komlos et al., 2008, Fang et al., 2009, Bopp et al., 2010, Williams et al., 2011, Alessi et al., 2014). With increasing distance, the water's U concentration and $\delta^{238}U$ continuously decrease. The relationship between concentration and $\delta^{238}U$ for a given mass of water moving through the system is given approximately by the Rayleigh distillationequation:

‰‰δ238U(t)=[δ238U(0)+1000‰]c(t)c(0)(∝-1)-1000‰

where t is time spent inside the reducing zone, $\delta^{238}U(0)$ and $c(0)$ are the inflowing water's U isotope composition and U concentration as it enters the reducing zone, $\delta^{238}U(t)$ and $c(t)$ give the same variables at time t, and α is the isotopic fractionation factor (defined above). Strictly speaking, this equation applies only to a closed batch reactor in which the product U(IV) does not interact chemically with the reactant U(VI). We assume here that the latter condition applies to the reducing parts of the system, where the U(IV) is not oxidizing and the rate of isotopic exchange between U(VI) and U(IV) is slow, as indicated by Wang et al. (2015b). The former condition is not strictly obeyed because a mass of water moving through an aquifer is not a closed system as dispersive mixing occurs. However, dispersive mixing does not destroy the validity of the Rayleigh model for simple systems, provided a somewhat smaller effective isotopic fractionation factor is used in place of the instrinsic fractionation factor (Abe and Hunkeler, 2006).

In a particular well, within the reducing zone, the relationship between $\delta^{238}U$ and U concentration over time should also conform to the Rayleigh model provided certain conditions are met. For instance, as the amount of reduction increases, the amount of U(VI) removed upstream of a given well increases, meaning the concentration at the given well decreases. While the Rayleigh equation applies strictly speaking to each volume of water moving through the reducing zone, each successive volume of water arriving at a given well experiences greater U(VI) reduction due to an increase in biomass and thus evolves to lower U concentrations and lower $\delta^{238}U$ following the same

Rayleigh function. This application of the equation is subject to certain conditions. The fractionation factor, α, must not vary over time. This is likely true if the conditions are near steady state, but it may not be true if the mechanism of reduction, or metabolic state of any microbes involved, changes. Also, the $\delta^{238}U$ and U concentration of the water entering the reducing zone must be constant. In this system, the inflowing water's $\delta^{238}U$ is essentially constant, as reflected in the background wells (Fig. 2a and b). The U concentration is not constant as a general rule, as it varies seasonally (±15%) and in response to bicarbonate injection (Fig. 2a and b). Accordingly, we do not expect simple Rayleigh models to fit all data in this system, but they approximate the data during certain time intervals when α and the inflowing concentration are nearly constant.

4.1.2.1. 'Super 8': short duration acetate only injection experiment

Plots of our data indicate several time intervals when the $\delta^{238}U$ vs. U(VI) relationships in wells CD01 and CD14 conform approximately to Rayleigh models with ε = +0.65‰ to +0.85‰ (α = 1.00065–1.00085). In 'Super 8', CD01 samples collected during the first 13 days of acetate injection, and during most of the recovery period (all but the first 16 days after injection ceased), conform to a Rayleigh model with an ε value of +0.85‰ and inflow U concentration of 0.90 μM (Fig. 3a). This concentration is reasonable for the earlier time interval. Although the background concentration in well CU01 was lower (starting at 0.66 μM and decreasing to 0.59 μM), the unintended HCO_3^- injection caused U(VI) desorption, with the CD01 concentration measured at 0.86 μM, and still increasing, at the onset of reduction. During the recovery period, CU01 concentrations (0.59–0.72 μM) were considerably lower than the best-fit model's inflow concentration, 0.90 μM (discussed below in Section 4.1.4). For instance, CD01 eventually attained a concentration of 1.0 μM, considerably higher that that in CU01, after it completely recovered from the acetate injection. Overall, during the two modeled time intervals in CD01, the results are consistent with a simple system, having roughly stable conditions, except for changing reduction rate, and no significant processes other than simple transport and reduction. The magnitude of isotopic fractionation, +0.85‰, is within the range obtained in laboratory U(VI) reduction experiments for a range of microbes (Basu et al., 2014, Stirling et al., 2015, Stylo et al., 2015). However, groundwater from the middle time span, with concentrations of 0.29 μM U or less, do not conform to the Rayleigh model, having much greater $\delta^{238}U$ for a given U concentration than predicted by early or late models. This departure from the model indicates a change in conditions or additional process not accounted for in the model as discussed below.

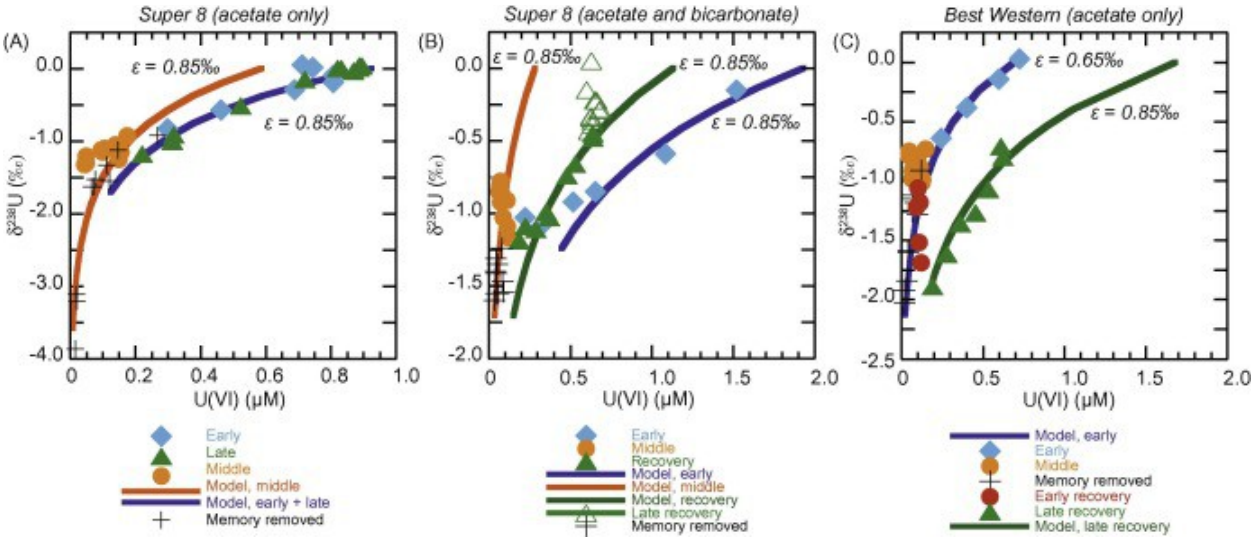

1. Download high-res image (410KB)
2. Download full-size image

Fig. 3. $\delta^{238}U$ vs. U as well as Rayleigh models for three separate experiments: (A) 'Super 8' (year 1), acetate only, (B) 'Super 8' (year 1), acetate and bicarbonate, and (C) 'Best Western' (year 2), acetate only. Diamonds are data from the early phase of acetate injection, triangles are data from the recovery phase, and circles are data from the middle phase based on U concentration changes (see Fig. 2). Lines represent Rayleigh distillation models; ε = +0.85‰ for all models except for the early phase model in (B), where it is +0.65‰. Inflow U concentrations for the models were chosen to represent those occurring at various times in the experiments (see text). Crosses represent calculated compositions of waters with a hypothetical "memory" component, 7 μg/L and $\delta^{238}U$ = 0‰, removed (see text).

4.1.2.2. 'Best Western': long duration acetate injection experiment

The second year's data from CD01 exhibit a similar pattern during the first part of the experiment, conforming to a Rayleigh model with an inflow concentration of 0.72 μM (equal to the concentration just prior to the onset of reduction) and an ε value of +0.65‰ (Fig. 3c). As in year one, this initial period of simple behavior is followed by a period of low concentrations in which the measured $\delta^{238}U$ values are greater than those of the model, for a given concentration.

During the latter part of the recovery phase, the data once again conform to a Rayleigh model, with ε = +0.85‰ (Fig. 3c). This value is required for the model to reproduce the observed slope of the data array. However, compared to data from the early time interval, these data are shifted strongly toward negative $\delta^{238}U$ values and/or toward higher U concentrations, indicating extraordinary conditions in the system. If an inflow

$\delta^{238}U$ value close to 0.0‰ is assumed, to match the upstream measurements, the model fits the data, but requires a high inflow concentration of about 1.7 μM (Fig. 3c). Background well CU01 concentration was 0.73 μM at that time, and desorption processes were not operating to augment it. Accordingly, some other process must be at work if such high inflow concentrations occurred (see below).

On the other hand, if an inflow concentration of 0.73 μM is assumed, then the data can be fit only by a model with an inflow $\delta^{238}U$ value of about −0.75‰. A strongly negative value such as this can only be attained if an additional process alters the $\delta^{238}U$ value of the water after it passes the upstream well, without greatly increasing its concentration. We considered exchange with adsorbed U(VI) as a potential process, but it requires adsorbed $\delta^{238}U$ values more negative than those of the groundwater—adsorption is not strong enough to drive the large shift required. This could occur only during the later part of the recovery phase, if the adsorbed U(VI) or fine-grained sediments (see below) retain some memory of more negative $\delta^{238}U$ values that came before. Thus, this effect does not provide a mechanism for attaining the most negative $\delta^{238}U$ values observed, before major $\delta^{238}U$ increase during the recovery phase. It also cannot explain the downward evolution of $\delta^{238}U$ values that occurred for about 100 days in the early recovery phase, after acetate injection ceased (Fig. 2c).

A third possible model for the strongly negative $\delta^{238}U$ values during the year 2 recovery phase in CD01 involves a larger isotopic fractionation. For example, at the time the most negative $\delta^{238}U$ value was observed, well CU01 had a concentration of 0.73 μM and a $\delta^{238}U$ of −0.01‰. Starting with that composition, an isotopic fractionation of ε = +1.50‰ is required to attain the −1.89‰ and 0.19 μM composition observed in well CD01 on day 198. Subsequent data require even greater fractionation; the day 273 sample requires ε = +2.1‰. These fractionations are much larger than those observed in laboratory experiments with a variety of microbes (Basu et al., 2014, Stirling et al., 2015, Stylo et al., 2015). Furthermore, they exceed measurements (Fujii et al., 2006, Wang et al., 2015b) and theoretical models (Abe et al., 2008) indicating equilibrium isotopic fractionation of about 1.3‰ between U(IV) and U(VI).

Kinetic isotope effects for reduction of elements other than U are generally observed to be substantially smaller than equilibrium isotopic fractionations (Canfield, 2001, Johnson and Bullen, 2004, Kritee et al., 2007, Basu and Johnson, 2012). Accordingly, the large fractionations of 1.5–2.1‰ required for simple Rayleigh models of the system during the recovery period are unreasonable. Overall, the strongly negative values observed in well CD01 during this period require an additional process acting in the aquifer (discussed below).

4.1.2.3. Acetate and bicarbonate injection

Well CD14 also has time intervals that fit Rayleigh models with ε = +0.85‰. Data from the first phase of reduction fit only roughly (Fig. 3b), because the bicarbonate injection on the west side of the plot caused inflow U concentrations to change greatly. The inflow concentration increased very strongly as U(VI) initially desorbed from solid surfaces, decreased slightly as the adsorbed U(VI) pool was depleted, then decreased very strongly after the bicarbonate injection ended. Nonetheless, the first three data points in CD14 roughly conform to a Rayleigh model with ε = +0.85‰ and an inflow concentration of 1.9 μM, the maximum concentration observed in CD14 before reduction caused it to decrease (Fig. 3b).

After the initial reduction phase, when U concentrations were low (~0.06 μM), anomalously high $\delta^{238}U$ values were observed (up to ~0.80‰), following the pattern of CD01 in both years. During the recovery phase, after U concentrations increased above 0.25 μM, the data conformed to a Rayleigh model with ε = +0.85‰ and inflow water with $\delta^{238}U$ = 0.0‰ and U concentration of 1.09 μM. This concentration is much greater than that observed in the upstream well CU03 during that time (0.64–0.78 μM). Alternatively, a model based on inflow water with $\delta^{238}U$ = −0.35‰ and U concentration of 0.71 μM is consistent with the data. As with the year 2 data from well CD01, an additional process not accounted for by a simple Rayleigh model is required.

4.1.3. “Memory” effects in the aquifer

Past research at the Rifle site has revealed that desorption of U(VI) is “kinetically inhibited” (Fox et al., 2012). Desorption of U(VI) in response to HCO_3^- injection was less intense and peak concentrations were delayed relative to an equilibrium surface complexation model. A multi-rate kinetic exchange model successfully reproduced observations by incorporating kinetically limited exchange between advecting waters and slow-flow zones bearing adsorption sites. This model is consistent with the presence of lenses of fine-grained materials in the aquifer. Best-fit exchange rates varied spatially, with mean exchange time scales varying from 1 to 14 days.

The existence of domains in the aquifer that exchange slowly with migrating groundwater suggest that the aquifer will retain a “memory” of past conditions that alters the U concentrations and $\delta^{238}U$ values of waters moving through the reducing zone. U(VI) inside the finer-grained domains would remain at high concentrations and near-zero $\delta^{238}U$ values for some time after the aquifer around them became reducing during the acetate injections. Trapped U(VI) inside silty domains close to wells CD01 and

CD14 would slowly advect or diffuse out and arrive at the wells relatively untouched by reduction.

Data from the periods with lowest U concentrations provide evidence for such a memory effect. The addition of a small mass of U(VI) with a near-zero $\delta^{238}U$ would have little effect on the water while the U concentration is high, but the observed $\delta^{238}U$ would be shifted to greater values as the dissolved U(VI) decreased in concentration and was thus more easily shifted. This is precisely what is observed. In both years' data series from CD01 and CD14, the system exhibits simple behavior and conforms to a Rayleigh model while concentrations are high, but the data shift away from the model toward higher $\delta^{238}U$ when concentrations become low.

A quantitative "unmixing" model provides a test of the hypothesis that a small mass of U(VI), with near-zero $\delta^{238}U$, emerged from silty domains and mixed with U(VI), that had evolved to low $\delta^{238}U$ and low concentration, as it passed through the reducing zone. The $\delta^{238}U$ value of the mixture (measured) can be related to the two mixed components via the equation:

$$\delta 238Umix=\delta 238Ureducedfreduced+\delta 238Umemory(1-freduced)(Y)$$

where "reduced" refers to U(VI) that migrated through the reducing zone to arrive at the well, "memory" refers to U(VI) derived from slow-flow zones close to the well, and $f_{reduced}$ is the fraction of U contributed by the reduced U(VI) component. To construct a simple model, we assumed the "memory" had a $\delta^{238}U$ value of 0.0‰, and solved for the composition of the reduced component with the memory component removed:

$$\delta 238Ureduced=\delta 238Umixfreduced(Z)$$

The mixing hypothesis predicts that $\delta^{238}U$ of this reduced component ($\delta^{238}U_{reduced}$) should match the Rayleigh model-predicted $\delta^{238}U$ when the memory component is removed (i.e., $\delta^{238}U_{memory}$ is 0.0‰), given the calculated U(VI) concentration of the reduced component The U(VI) concentration of the reduced component is calculated from the measured U(VI) concentration and the only free parameter, the U(VI) concentration of the memory component.

In both years' data series from CD01 and CD14, removal of a memory component from the measured water samples yields $\delta^{238}U$ values that do coincide with the Rayleigh models. Tuning of the U(VI) of the memory component revealed a memory component providing 0.03 μM of U(VI) with $\delta^{238}U$ = 0‰, constant over time, yields good results for all three data series. This memory component represents 16–66% of the total observed concentration. The unmixing model (Eq. Y) was used to remove this memory component from the low concentration samples in the middle of each data series. The calculated reduced components form arrays of $\delta^{238}U$ vs. concentration that are close to

Rayleigh models appropriate for those times periods (Fig. 3). In other words, when the memory component is removed, the remaining U concentration and $\delta^{238}U$ are consistent with simple transport-reduction models describing the evolution of waters in the reducing zone. For example, for the middle time interval of year one in well CD01, we constructed a best-estimate Rayleigh model to approximate expected groundwater compositions in the reducing zone for this time interval. Inflow concentration and $\delta^{238}U$ were set at 0.59 μM and 0.0‰, respectively, to match the composition of upstream well CU01, and ε was set at 0.85‰ to match the value that fits several time intervals in this study (see above). The results of the unmixing calculations are plotted in Fig. 3a. Whereas the measured samples fall in a cluster far from the best-estimate Rayleigh model, when the memory component is removed, the samples conform closely to the model. The results are similar for CD01, year 2 (Fig. 3c). For the CD14 case, the calculated compositions plot along a Rayleigh trend with a low inflow concentration (Fig. 3b), as expected due to strong adsorption as surface sites were repopulated after the HCO_3^- injection ended.

Overall, the anomalously high $\delta^{238}U$ values observed in the middle periods of all three data series are consistent with a simple model involving a small amount of “memory” of past conditions. We expect the actual kinetically limited exchange process in the aquifer to be more complex (e.g., waning with time) but to first order, the model appears to be a good approximation. In the simple analysis we present here, the memory effect is apparent only when the dissolved U concentration is small. However, a more accurate representation of exchange processes, as part of a more detailed and complex reaction-transport model for the U isotope data presented here, would provide a more rigorous data interpretation.

4.1.4. Post-acetate oxidation

After the acetate injection ceased, small amounts of dissolved oxygen and/or other oxidants in the inflowing water may have oxidized some of the recently formed U(IV) precipitates to U(VI). From the concentration data alone, it is not clear if U(IV) oxidation occurred. If it did, it would have occurred initially only on the leading edge of the reducing zone, because oxidants could not penetrate far into it before being consumed by residual reducing power remaining from the acetate injection, including continued microbial activity and reduced solids such as biomass, Fe(II)-bearing minerals, and sulfide minerals that were formed during the acetate injection (Williams et al., 2011). Any U(VI) generated at the oxidation front would thus be carried into the remaining reducing zone and would likely be reduced again, partially or completely, by

the residual reducing power. Accordingly, the U(VI) in groundwater sampled at wells CD01 and CD14 may be the end product resulting from addition of oxidized U(IV) to waters migrating from upstream, followed by varying degrees of subsequent U(VI) reduction.

We hypothesize that this scenario, with U(IV) oxidation at the upstream side of the reduced zone, and U(VI) reduction continuing in the downstream side of the reduced zone, could have produced the anomalous values observed in well CD01 during the year 2 recovery phase (Fig. 3c). As discussed above, the observed array of points from the late recovery phase conforms to a simple Rayleigh model, but requires the inflowing water to have a very high U concentration. If oxidation of U(IV) occurred in the upstream part of the reduced zone, the generated U(VI) would augment that of the inflowing water, leading to the required high U concentrations at the upstream side of the reducing zone. As the water migrated deeper into the reduced zone, ongoing U(VI) reduction could produce the lower concentrations and strongly negative observed $\delta^{238}U$ values (Fig. 3c).

Although the oxidized U(IV) must have had positive $\delta^{238}U$ values, they would not be strongly positive. We estimated the range of possible $\delta^{238}U$ values for the groundwater in the zone of U(IV) oxidation, based on the apparent isotopic fractionation factor for the reduction process that generated the U(IV), the $\delta^{238}U$ value of inflowing water, and the expected spatial pattern in the $\delta^{238}U$ value of precipitated U(IV). We assumed that oxidation of solid U(IV) phases involves no isotopic fractionation, based on an experimental study (Wang et al., 2015a). With $\delta^{238}U = 0.0‰$ for the inflowing water, the $\delta^{238}U$ of the (IV) precipitated at the upstream edge of the U(IV)-bearing zone would have been about 0.65‰, assuming the isotopic fractionation was +0.65‰ (the apparent value derived from the preceding reduction phase). Importantly, the U(IV) precipitates must have decreased in $\delta^{238}U$ with increasing distance downstream, following the spatial trend of the parent waters, and the $\delta^{238}U$ value of the U released via U(IV) oxidation to waters traveling downstream would be a spatially integrated average of the U(IV) acquired. During the time interval when U(VI) reduction was strong, U(VI) was removed quickly from inflowing waters, and thus $\delta^{238}U$ of both the dissolved U(VI) and the precipitated U(IV) decreased strongly over a short distance (e.g., <0.5 m). Essentially all of the incoming U(VI), with $\delta^{238}U$ close to 0.0‰, would have been reduced in this zone and deposited as U(IV), which therefore would have a spatially averaged $\delta^{238}U$ close to 0.0‰. Later, if U(IV) oxidation became strong, oxidants would likely penetrate significantly into this zone, releasing U(IV) with $\delta^{238}U$ values ranging from +0.65‰ at the upstream side to much lower values deeper into the zone. Accordingly, we expect the

$\delta^{238}U$ value of the total U(VI) acquired by oxidation to be considerably less than +0.65‰, and possibly close to 0.0‰ if the oxidants penetrated across most of the zone of former U(IV) precipitation.

Mixture of this U(VI) with that dissolved in water migrating from upstream would result in a $\delta^{238}U$ value not much greater than 0.0‰. For example, if upstream water containing 0.84 μM U(VI) with $\delta^{238}U$ = 0.0‰ acquired 0.84 μM additional U(VI) with $\delta^{238}U$ = 0.40‰ via U(IV) oxidation, the water would then have 1.7 μM U(VI) with $\delta^{238}U$ = 0.20‰. Similarly, water with a total U concentration of 2.5 μM could be produced with $\delta^{238}U$ = 0.27‰. We cannot determine the exact composition of waters resulting from U(IV) oxidation during the experiments, because it is controlled by several variables. However, we assert that oxidation could readily produce high U concentrations, with slightly positive $\delta^{238}U$ values.

The anomalous data observed in CD01 during the year two recovery phase conform to a model based on U(IV) oxidation in the upstream side of the U(IV)-bearing zone. A Rayleigh model shown in Fig. 3c, based on ε = +0.85‰ and inflow $\delta^{238}U$ and U concentration values of +0.30‰ and 2.5 μM, respectively, approximates the observed data array. These values are reasonable, but are non-unique; a closely similar Rayleigh trend can be produced using initial $\delta^{238}U$ and U concentration values of +0.40‰ and 2.9 μM, respectively. The uncertainty in ε, determined from the scatter of the points about the best-fit line via standard linear estimation methods, is 0.19‰ (2 S.E.). In general, U(IV) oxidation could produce inflow values in this range, and can produce a model that fits the data. The extent of reduction required is 93–94% of inflowing U(VI) reduced prior to the water's arrival at CD01. This is high, but not unreasonable. Similar extents of reduction probably occurred earlier in the year 2 experiments, but as discussed above and illustrated with the unmixing model, highly negative $\delta^{238}U$ values were obscured by the memory of earlier, higher $\delta^{238}U$ values.

Overall, these fits show that U(IV) oxidation upstream, combined with continued strong reduction downstream, could have caused the anomalous data trend. We are unable to find other reasonable models that can reproduce the data. As described above, a simple model involving only transport and reduction requires isotopic fractionation much stronger than current experiments and theory allow. U(VI) exchange with an adsorbed pool, or "memory" stored in fine grained sediments, cannot explain the data because it cannot act to shift $\delta^{238}U$ lower except after $\delta^{238}U$ begins to increase strongly. Furthermore, such memory effects appear to be small, affecting only U(VI)-poor waters. Given the known processes occurring in this system, the only other process that could greatly impact the dissolved U(VI) is oxidation.

It appears that smaller amounts of U(IV) oxidation may have impacted the data from CD14 and CD01 in year one. In both cases, the data conform approximately to a Rayleigh model having an inflow U(VI) greater than the concentration observed in upstream wells CU01 and CU03. Similar to the CD01 year 2 case, such a shift toward greater concentration could have been caused by oxidation of U(IV). Additional evidence that oxidation occurred during year one recovery is provided by the higher concentrations for well CD01 as compared to the upstream well CU01 (Fig. 2a).

4.1.5. Limitations of this model

The conceptual model presented above accounts for expected processes in the aquifer and suggests that $\delta^{238}U$ values respond in a coherent way to those processes. Given the available detailed characterization of the experimental plot and processes within it (Long et al., 2015) a groundwater reactive transport model that quantitatively simulates the processes governing $\delta^{238}U$ values is achievable and would provide a better assessment of the strengths and limitations of $\delta^{238}U$ data in this and other groundwater systems. Such a model is currently planned as a future study.

4.2. Apparent isotopic fractionation factors: comparison to previous field and laboratory experiments

The apparent ε values we infer from our data range from +0.65‰ to +0.85‰ and are close to those reported for microbial U(VI) reduction by various microbial strains in laboratory experiments (0.68–0.99‰) (Basu et al., 2014, Stirling et al., 2015, Stylo et al., 2015). According to previous work at this site, the observed decrease in U concentration results from microbial reduction (Williams et al., 2011, Zhuang et al., 2011, Wilkins et al., 2013, Long et al., 2015). This reinforces the simple interpretation implied by our Rayleigh models; during some time intervals the data are consistent with straightforward advection and microbial reduction of U(VI), with relatively minor roles for other processes.

The apparent magnitude of fractionation observed in this study is considerably larger than an earlier estimate of 0.46‰ calculated for the 2009 Rifle biostimulation experiment in plot A (Bopp et al., 2010). However, the isotopic analyses in that study had greater uncertainty (±0.12‰) and were relatively sparse, with eight analyses of pre-reduction samples, nine analyses from the middle part of the experiment when U(VI) reduction was strong (>70% removal), and only two from times of moderate reduction. We expect the $\delta^{238}U$ results from the middle part of the experiment, when U concentration was very low, were impacted by the memory effect that is apparent in all

three of our data series, and are thus not good indicators of the magnitude of fractionation. Furthermore, one of the Bopp et al. (2010)moderate reduction samples had a $\delta^{238}U$ value with a significant negative deviation from the Rayleigh model used to calculate the magnitude of fractionation. Taken alone, this data point fits a Rayleigh model with a fractionation of 0.86‰. Generally, the results of the Bopp et al. (2010) study are quite similar to our data from CD01 in year one, the most directly comparable case: $\delta^{238}U$ decreased by about 1.0‰, then remained nearly constant during the middle period of the experiment. Accordingly, we suggest that the actual isotopic fractionation occurring in the 2009 plot A experiment was likely greater than the value reported in Bopp et al. (2010), because the memory effects apparent in our data set probably affected their results as well.

Abiotic reduction of U(VI) has been shown, in recent laboratory studies, to impart little or no U isotope fractionation (Rademacher et al., 2006, Stirling et al., 2007, Grimm, 2014, Stylo et al., 2015) or isotopic fractionation in opposition to nuclear volume fractionation (Stylo et al., 2015). Assuming these laboratory results apply to the Rifle site, most or all of the U(VI) reduction we observe must have been directly mediated by microbes. If reduction had proceeded dominantly via reaction with dissolved Fe(II), Fe(II)-bearing solid phases, dissolved sulfide, or solid sulfide phases, all of which are known to be generated by microbial action during the acetate injections, isotopic fractionation would be been nearly zero (Stylo et al., 2015). This conclusion is especially significant during the long recovery phase of CD01 in year two. U concentrations remained low long after acetate amendment ceased, indicating that the built-up reducing power of the aquifer continued to reduce U(VI). During this time interval, we observed extremely negative $\delta^{238}U$ values, and it appears that microbial action remained the dominant reduction mechanism, despite the low acetate concentrations that would tend to slow microbial reduction and the expected presence of sulfide minerals that are known to reduce U(VI) (Hua et al., 2006, Boonchayaanant et al., 2010, Williams et al., 2011). Our field data provide an example of how Stylo et al. (2015)results can be used to distinguish between reductions occurring via microbial or abiotic pathways.

4.3. Implications for $^{238}U/^{235}U$ ratio studies at U remediation sites

The results of this study illustrate both the unique capabilities and limitations of $^{238}U/^{235}U$ ratio measurements. First, the results of this study suggest that microbial reduction in field settings induces consistent isotopic fractionation similar to that observed in laboratory experiments (Basu et al., 2014, Stirling et al., 2015, Stylo et al., 2015). This fractionation factor is approximately double that extracted from the relatively sparse $^{238}U/^{235}U$ ratio data set of Bopp et al. (2010). Accordingly, $^{238}U/^{235}U$ ratio

measurements show promise as indicators of microbial U(VI) reduction in groundwater systems. Importantly, $^{238}U/^{235}U$ ratio shifts occur primarily as a result of microbial U(VI) reduction, and thus provide direct evidence for biotic reduction (Stylo et al., 2015). In contrast, use of dissolved U concentrations to infer reduction involves interpretation of spatial or temporal changes in concentrations after adsorption processes have been accounted for.

In the case of the Rifle experiments, the careful experimental design, the simplicity of the system, and the detailed spatial and temporal U concentration measurements provide for a very controlled setup. The occurrence of reduction is obvious from concentration data alone and it can be quantified reasonably well (Long et al., 2015). However, in many more common U contamination sites, groundwater flow and geochemical variations are more complex, sampling points are sparse, and reduction is not as abrupt or as strong. Sorting out the effects of mixing and adsorption on U concentrations is likely much more difficult. In such settings, observed shifts in dissolved U(VI) $^{238}U/^{235}U$ ratios can still provide straightforward evidence of U(VI) reduction. The present study makes use of the detail of the Rifle experiments to demonstrate that $^{238}U/^{235}U$ ratio measurements respond in a straightforward way to microbial reduction in the field. This knowledge can now be applied to other sites that are less intensively instrumented and sampled, where reduction is more difficult to detect and/or quantify via concentration changes.

In a more general sense, $^{238}U/^{235}U$ ratio measurements provide complementary information not contained in U concentration data alone, and the two data types can be used together to reveal processes not fully constrained by either one. One example of this is our inference that oxidation of U(IV) occurred at the upstream side of the reducing zone after acetate injection ended in year 2. The strongly negative $\delta^{238}U$ values indicate very strong reduction, and because the U concentration is too high to be explained by a simple transport-reduction scenario with such strong reduction, we infer that an additional source of U(VI) was required.

The present study also shows that $^{238}U/^{235}U$ ratio data do not always provide a straightforward indication of the extent of U(VI) reduction. In the times of strong reduction and low U concentration, we found that a mixing model was required to account for a local “memory” component, in addition to the simple Rayleigh equation used to model advection and reduction of U(VI) from upstream. More complex reactive transport models that simultaneously account for advection, reduction, dispersion, sorption, and oxidation would provide a means to interpret the data in cases where sites are characterized well enough to constrain these processes.

5. Conclusions

A highly detailed $^{238}U/^{235}U$ ratio data set from the Rifle IFRC biostimulation experiments of 2010 and 2011 in Plot C indicates that $^{238}U/^{235}U$ ratios decrease consistently in response to microbial U(VI) reduction, which is well constrained by spatially and temporally dense U concentration measurements. During some time intervals, the $^{238}U/^{235}U$ ratio data are consistent with a simple advection-reduction model; data fall along Rayleigh distillationtrends. These trends indicate isotopic fractionation of +0.65‰ to +0.85‰, similar to that observed in recent laboratory studies of microbial U(VI) reduction. The results are also consistent with the relatively sparse $^{238}U/^{235}U$ ratio data set from an earlier experiment in a different area of the Rifle site (Bopp et al., 2010). In light of recent findings that abiotic U(VI) reduction induces little or no isotopic fractionation (Rademacher et al., 2006, Stirling et al., 2007, Grimm, 2014, Stylo et al., 2015), or isotopic fractionation in the opposite direction (Stylo et al., 2015), the large $^{238}U/^{235}U$ ratio shifts observed at Rifle indicate that U(VI) reduction must occur via direct microbial activity with little if any reduction occurring by abiotic processes.

During times of strong U(VI) reduction and low U concentrations in wells impacted by the biostimulation, the $^{238}U/^{235}U$ ratio data suggest the presence of a U(VI) component with a near-zero $\delta^{238}U$ value, in addition to the highly negative U(VI) arriving at the wells after passage through the zone of intense reduction. The extra component is likely derived from kinetically inhibited U(VI) exchange between faster-flowing aquifer domains and fine-grained domains in the aquifer, a process previously identified at the Rifle site by Fox et al. (2012).

During time intervals when U concentrations recovered after the cessation of acetateinjection, the relationships between U concentration and $\delta^{238}U$ suggest the occurrence of U(IV) oxidation at the upstream edge of the reducing zone, and the subsequent partial reduction of the produced U(VI) as it migrated deeper into the reducing zone.

Our study supports the use of $^{238}U/^{235}U$ ratios as a tool for evaluating the efficacy of biostimulation and potentially other remedial strategies employed at the Rifle IFRC and similar sites. The results demonstrate the ability of $^{238}U/^{235}U$ ratios to detect U reductive immobilization in the subsurface, distinguishing reduction from temporary removal processes such as sorption, and suggest quantifying the extent of U reduction is possible. Further, the results identify departures from Rayleigh behavior in groundwater systems arising from the presence of adsorbed species and show that isotope data are sensitive to the onset of oxidation after biostimulation ends, even in the case where

reduction continues to remove uranium downstream. These results have important implications for the interpretation of U isotopes at field sites. These field results may be used to calibrate reactive transport models, which take into account the complex and heterogeneous environments of real field sites. Ultimately, these models will facilitate the prediction of uranium fate at remediated sites.

Acknowledgements

We thank Alison Montgomery and Mark Robbins for help collecting groundwater samples and Joern Larsen for quantifying dissolved U concentrations in groundwater samples. Funding was provided through the U.S. Department of Energy (DOE), Office of Science, Office of Biological and Environmental Research under contracts DE-SC0006755 (University of Illinois at Urbana-Champaign) and DE-AC02-05CH11231 (Lawrence Berkeley National Laboratory; operated by the University of California). This material is based upon work equally supported through the Integrated Field Research Challenge Site (IFRC) at Rifle, Colorado and the Lawrence Berkeley National Laboratory's Sustainable Systems Scientific Focus Area. We are greatly appreciative of the constructive reviews by three anonymous reviewers and to Claudine Stirling for editorial handling.

References

Abe and Hunkeler, 2006

Y. Abe, D. Hunkeler**Does the Rayleigh equation apply to evaluate field isotope data in contaminant hydrogeology?**

Environ. Sci. Technol., 40 (2006), pp. 1588-1596

CrossRefView Record in Scopus

Abe et al., 2008

M. Abe, T. Suzuki, Y. Fujii, M. Hada, K. Hirao**An ab initio molecular orbital study of the nuclear volume effects in uranium isotope fractionations**

J. Chem. Phys., 129 (2008), p. 164309

CrossRef

Alessi et al., 2014

D.S. Alessi, J.S. Lezama-Pacheco, N. Janot, E.I. Suvorova, J.M. Cerrato, D.E. Giammar, J.A.Davis, P.M. Fox, K.H. Williams, P.E. Long, K.M. Handley, R. Bernier-Latmani, J.R. Bargar**Speciation and reactivity of uranium products formed during in situ bioremediation in a shallow alluvial aquifer**

Environ. Sci. Technol., 48 (2014), pp. 12842-12850

CrossRefView Record in Scopus

Andersen et al., 2014

M.B. Andersen, S.J. Romaniello, D. Vance, S.H. Little, R. Herdman, T.W. Lyons**A modern framework for the interpretation of $^{238}U/^{235}U$ in studies of ancient ocean redox**

Earth Planet. Sci. Lett., 400 (2014), pp. 184-194

ArticleDownload PDFView Record in Scopus

Anderson et al., 2003

R. Anderson, H. Vrionis, I. Ortiz-Bernad**Stimulating the in situ activity of *Geobacter* species to remove uranium from the groundwater of a uranium-contaminated aquifer**

Appl. Environ. Microbiol., 69 (2003), pp. 5884-5891

CrossRefView Record in Scopus

Basu and Johnson, 2012

A. Basu, T.M. Johnson**Determination of hexavalent chromium reduction using Cr stable isotopes: isotopic fractionation factors for permeable reactive barrier materials**

Environ. Sci. Technol., 46 (2012), pp. 5353-5360

CrossRefView Record in Scopus

Basu et al., 2014

A. Basu, R.A. Sanford, T.M. Johnson, C.C. Lundstrom, F.E. Löffler**Uranium isotopic fractionation factors during U(VI) reduction by bacterial isolates**

Geochim. Cosmochim. Acta, 136 (2014), pp. 100-113

ArticleDownload PDFView Record in Scopus

Bigeleisen, 1996

J. Bigeleisen**Nuclear size and shape effects in chemical reactions. Isotope chemistry of the heavy elements**

J. Am. Chem. Soc., 118 (1996), pp. 3676-3680

CrossRefView Record in Scopus

Boonchayaanant et al., 2010

B. Boonchayaanant, B. Gu, W. Wang, M.E. Ortiz, C.S. Criddle**Can microbially-generated hydrogen sulfide account for the rates of U(VI) reduction by a sulfate-reducing bacterium?**

Biodegradation, 21 (2010), pp. 81-95

CrossRef

Bopp et al., 2009

C.J. Bopp, C.C. Lundstrom, T.M. Johnson**Variations in $^{238}U/^{235}U$ in uranium ore deposits: isotopic signatures of the U reduction process?**

Geology, 37 (2009), pp. 611-614

CrossRefView Record in Scopus

Bopp et al., 2010

C.J. Bopp, C.C. Lundstrom, T.M. Johnson, R.A. Sanford, P.E. Long, K.H. Williams**Uranium $^{238}U/^{235}U$ isotope ratios as indicators of reduction: results from an in situ biostimulation experiment at Rifle, Colorado, USA**

Environ. Sci. Technol., 44 (2010), pp. 5927-5933
CrossRefView Record in Scopus

Brennecka et al., 2010

G.A. Brennecka, L.E. Borg, I.D. Hutcheon, M.A. Sharp, A.D. Anbar**Natural variations in uranium isotope ratios of uranium ore concentrates: Understanding the $^{238}U/^{235}U$ fractionation mechanism**
Earth Planet. Sci. Lett., 291 (2010), pp. 228-233
ArticleDownload PDFView Record in Scopus

Brennecka et al., 2011

G. Brennecka, L. Wasylenki, J. Bargar**Uranium isotope fractionation during adsorption to Mn-oxyhydroxides**
Environ. Sci. Technol., 45 (2011), pp. 1370-1375
CrossRefView Record in Scopus

Canfield, 2001

D.E. Canfield**Biogeochemistry of sulfur isotopes**
J.W. Valley, D.R. Cole (Eds.), Stable Isotope Geochemistry, Mineralogical Society of America and Geochemical Society, Washington, D.C. (2001), pp. 607-636
CrossRefView Record in Scopus

DOE, 1999

DOE (1999) Final Site Observational Work Plan for the UMTRA Project Old Rifle Site. In DOE (ed.), Grand Junction, CO, pp. 122.

Fang et al., 2009

Y. Fang, S.B. Yabusaki, S.J. Morrison, J.P. Amonette, P.E. Long**Multicomponent reactive transport modeling of uranium bioremediation field experiments**
Geochim. Cosmochim. Acta, 73 (2009), pp. 6029-6051
ArticleDownload PDFView Record in Scopus

Florence et al., 1

T.M. Florence, G.E. Batley, A. Ekstrom, J.J. Fardy, Y.J. Farrar**Separation of uranium isotopes by uranium(IV)–uranium(VI) chemical exchange**
J. Inorg. Nucl. Chem., 37 (1975), pp. 1961-1966
ArticleDownload PDFView Record in Scopus

Fox et al., 2012

P.M. Fox, J.A. Davis, M.B. Hay, M.E. Conrad, K.M. Campbell, K.H. Williams, P.E. Long**Rate-limited U(VI) desorption during a small-scale tracer test in a heterogeneous uranium-contaminated aquifer**
Water Resour. Res., 48 (2012), p. W05512, 10.1029/2011WR011472

Fujii et al., 2006

Y. Fujii, N. Higuchi, Y. Haruno, M. Nomura, T. Suzuki**Temperature dependence of isotope effects in uranium chemical exchange reactions**
J. Nucl. Sci. Technol., 43 (2006), pp. 400-406
CrossRefView Record in Scopus

Grimm, 2014

T.R. Grimm**Isotopic study of uranium: determining the isotopic fractionation of uranium during abiotic reduction with iron(II)**
Geology (2014), p. 52
University of Illinois at Urbana-Champaign, Urbana, IL
View Record in Scopus

Hinojosa et al., 2

J.L. Hinojosa, C.H. Stirling, M.R. Reid, C.M. Moy, G.S. Wilson**Trace metal cycling and 238U/235U in New Zealand's fjords: Implications for reconstructing global paleoredox conditions in organic-rich sediments**
Geochim. Cosmochim. Acta, 179 (2016), pp. 89-109
ArticleDownload PDFView Record in Scopus

Holmden et al., 2

C. Holmden, M. Amini, R. Francois**Uranium isotope fractionation in Saanich Inlet: a modern analog story of a paleoredox tracer**
Geochim. Cosmochim. Acta, 153 (2015), pp. 202-215
ArticleDownload PDFView Record in Scopus

Holmes et al., 20

D.E. Holmes, R.A. O'Neil, H.A. Vrionis, L.A. N'Guessan, I. Ortiz-Bernad, M.J. Larrahondo, L.A. A dams, J.A. Ward, J.S. Nicoll, K.P. Nevin, M.A. Chavan, J.P. Johnson, P.E. Long, D.R. Lovley**Subs urface clade of Geobacteraceae that predominates in a diversity of Fe(III)-reducing subsurface environments**
ISME J., 1 (2007), pp. 663-677
CrossRefView Record in Scopus

Hua et al., 2006

B. Hua, H. Xu, J. Terry, B. Deng**Kinetics of uranium(VI) reduction by hydrogen sulfide in anoxic aqueous systems**
Environ. Sci. Technol., 40 (2006), pp. 4666-4671
CrossRefView Record in Scopus

Hyslop and Whit

N.P. Hyslop, W.H. White**Estimating precision using duplicate measurements**
J. Air Waste Manag. Assoc., 59 (2009), pp. 1032-1039
CrossRefView Record in Scopus

Jaffey et al., 197

A. Jaffey, K. Flynn, L. Glendenin, W. Bentley, A. Essling**Precision measurement of half-lives and specific activities of ^{235}U and ^{238}U**
Phys. Rev. C, 4 (1971), pp. 1889-1906
CrossRefView Record in Scopus

Johnson and Bu

T.M. Johnson, T.D. Bullen**Mass-dependent fractionation of selenium and chromium isotopes in low-temperature environments**
C.M. Johnson, B.L. Beard, F. Albarede (Eds.), Geochemistry of Non-traditional Stable Isotopes (2004), pp. 289-317
Washington, D.C.
CrossRefView Record in Scopus

Komlos et al., 20

J. Komlos, A. Peacock, R.K. Kukkadapu, P.R. Jaffé**Long-term dynamics of uranium reduction/reoxidation under low sulfate conditions**
Geochim. Cosmochim. Acta, 72 (2008), pp. 3603-3615
ArticleDownload PDFView Record in Scopus

Kritee et al., 200

K. Kritee, J.D. Blum, M.W. Johnson, B.A. Bergquist, T. Barkay**Mercury stable isotope fractionation during reduction of Hg(II) to Hg(0) by mercury resistant microorganisms**
Environ. Sci. Technol., 41 (2007), pp. 1889-1895
CrossRefView Record in Scopus

Langmuir, 1997

D. Langmuir**Aqueous Environmental Geochemistry**

Prentice Hall (1997)

Long et al., 2015

P.E. Long, K.H. Williams, J.A. Davis, P.M. Fox, M.J. Wilkins, S.B. Yabusaki, Y. Fang, S.R.Waichler, E.S.F. Berman, M. Gupta, D.P. Chandler, C. Murray, A.D. Peacock, L. Giloteaux, K.M. Handley, D.R. Lovley, J.F. Banfield**Bicarbonate impact on U(VI) bioreduction in a shallow alluvial aquifer**

Geochim. Cosmochim. Acta, 150 (2015), pp. 106-124

ArticleDownload PDFView Record in Scopus

Lovley et al., 199

D.R. Lovley, E.J.P. Phillips, Y.A. Gorby, E.R. Landa**Microbial reduction of uranium**

Nature, 350 (1991), pp. 413-416

CrossRefView Record in Scopus

Montoya-Pino et

C. Montoya-Pino, S. Weyer, A.D. Anbar, J. Pross, W. Oschmann, B. van de Schootbrugge, H.W. Arz**Global enhancement of ocean anoxia during Oceanic Anoxic Event 2: a quantitative approach using U isotopes**

Geology, 38 (2010), pp. 315-318

CrossRefView Record in Scopus

Murphy et al., 20

M.J. Murphy, C.H. Stirling, A. Kaltenbach, S.P. Turner, B.F. Schaefer**Fractionation of $^{238}U/^{235}U$ by reduction during low temperature uranium mineralisation processes**

Earth Planet. Sci. Lett., 388 (2014), pp. 306-317

ArticleDownload PDFView Record in Scopus

Newsome et al.,

L. Newsome, K. Morris, J.R. Lloyd**The biogeochemistry and bioremediation of uranium and other priority radionuclides**

Chem. Geol., 363 (2014), pp. 164-184

ArticleDownload PDFView Record in Scopus

Nomura et al., 19

M. Nomura, N. Higuchi, T. Fujii**Mass dependence of uranium isotope effects in the U(IV)–U(VI) exchange reaction**

J. Am. Chem. Soc., 118 (1996), pp. 9127-9130

CrossRefView Record in Scopus

Noordmann et al

J. Noordmann, S. Weyer, C. Montoya-Pino, O. Dellwig, N. Neubert, S. Eckert, M.Paetzel, M.E. Bottcher**Uranium and molybdenum isotope systematics in modern euxinic basins: case studies from the central Baltic Sea and the Kyllaren fjord (Norway)**

Chem. Geol., 396 (2015), pp. 182-195

ArticleDownload PDFView Record in Scopus

Rademacher et a

L.K. Rademacher, C.C. Lundstrom, T.M. Johnson, R.A. Sanford, J. Zhao, Z. Zhang**Experimentally determined uranium isotope fractionation during reduction of hexavalent U by bacteria and zerovalent iron**
Environ. Sci. Technol., 40 (2006), pp. 6943-6948
CrossRefView Record in Scopus

Schauble, 2004

E.A. Schauble**Applying stable isotope fractionation theory to new systems**
C.M. Johnsos, B.L. Beard, F. Albarede (Eds.), Geochemistry of Non-traditional Stable Isotopes, 55(2004), pp. 65-111
CrossRefView Record in Scopus

Schauble, 2007

E.A. Schauble**Role of nuclear volume in driving equilibrium stable isotope fractionation of mercury, thallium, and other very heavy elements**
Geochim. Cosmochim. Acta, 71 (2007), pp. 2170-2189
ArticleDownload PDFView Record in Scopus

Shiel et al., 2013

A.E. Shiel, P.G. Laubach, T.M. Johnson, C.C. Lundstrom, P.E. Long, K.H. Williams**No measurable changes in $^{238}U/^{235}U$ due to desorption–adsorption of U(VI) from groundwater at the Rifle, Colorado, integrated field research challenge site**
Environ. Sci. Technol., 47 (2013), pp. 2535-2541
CrossRefView Record in Scopus

Stewart et al., 20

B.D. Stewart, M.A. Mayes, S. Fendorf**Impact of uranyl−calcium−carbonato complexes on uranium(VI) adsorption to synthetic and natural sediments**
Environ. Sci. Technol., 44 (2010), pp. 928-934
CrossRefView Record in Scopus

Stirling et al., 20

C.H. Stirling, A.N. Halliday, D. Porcelli**In search of live ^{247}Cm in the early solar system**
Geochim. Cosmochim. Acta, 69 (2005), pp. 1059-1071
ArticleDownload PDFView Record in Scopus

Stirling et al., 20

C.H. Stirling, A.N. Halliday, E.-K. Potter, M.B. Andersen, B. Zanda**A low abundance of ^{247}Cm in the early solar system and implications for r-process nucleosynthesis**
Earth Planet. Sci. Lett., 251 (2006), pp. 386-397
ArticleDownload PDFView Record in Scopus

Stirling et al., 20

C.H. Stirling, M.B. Andersen, E.-K. Potter, A.N. Halliday**Low temperature isotopic fractionation of uranium**

Earth Planet. Sci. Lett., 264 (2007), pp. 208-225
ArticleDownload PDFView Record in Scopus

Stirling et al., 201

C.H. Stirling, M.B. Andersen, R. Warthmann, A.N. Halliday**Isotope fractionation of ^{238}U and ^{235}U during biologically-mediated uranium reduction**
Geochim. Cosmochim. Acta, 163 (2015), pp. 200-218
ArticleDownload PDFView Record in Scopus

Stylo et al., 2015

M. Stylo, N. Neubert, Y. Wang, N. Monga, S.J. Romaniello, S. Weyer, R. Bernier-Latmani**Uranium isotopes fingerprint biotic reduction**
Proc. Natl. Acad. Sci. USA (2015)

Wang et al., 2015a

X. Wang, T.M. Johnson, C.C. Lundstrom**Isotope fractionation during oxidation of tetravalent uranium by dissolved oxygen**
Geochim. Cosmochim. Acta, 150 (2015), pp. 160-170
ArticleDownload PDFView Record in Scopus

Wang et al., 2015b

X. Wang, T.M. Johnson, C.C. Lundstrom**Low temperature equilibrium isotope fractionation and isotope exchange kinetics between U(IV) and U(VI)**
Geochim. Cosmochim. Acta (2015)

Weyer et al., 2008

S. Weyer, A.D. Anbar, A. Gerdes, G.W. Gordon, T.J. Algeo, E.A. Boyle**Natural fractionation of U-238/U-235**
Geochim. Cosmochim. Acta, 72 (2008), pp. 345-359
ArticleDownload PDFView Record in Scopus

Wilkins et al., 2013

M.J. Wilkins, K.C. Wrighton, C.D. Nicora, K.H. Williams, L.A. McCue, K.M. Handley, C.S.Miller, L. Giloteaux, A.P. Montgomery, D.R. Lovley, J.F. Banfield, P.E. Long, M.S. Lipton**Fluctuations in species-level protein expression occur during element and nutrient cycling in the subsurface**
PLoS One, 8 (2013)

Williams et al., 2011

K.H. Williams, P.E. Long, J.A. Davis, M.J. Wilkins, N&apos, A.L. Guessan, C.I. Steefel, L.Yang, D. Newcomer, F.A. Spane, L.J. Kerkhof, L. McGuinness, R. Dayvault, D.R. Lovely**Acetate availability and its influence on sustainable bioremediation of uranium-contaminated groundwater**
Geomicrobiol. J., 28 (2011), pp. 519-539
CrossRefView Record in Scopus

Zachara et al., 2013

J.M. Zachara, P.E. Long, J. Bargar, J.A. Davis, P. Fox, J.K. Fredrickson, M.D. Freshley, A.E.Konopka, C. Liu, J.P. McKinley, M.L. Rockhold, K.H. Williams, S.B. Yabusaki**Persistence of uranium groundwater plumes: contrasting mechanisms at two DOE sites in the groundwater-river interaction zone**

J. Contam. Hydrol., 147 (2013), pp. 45-72

ArticleDownload PDFView Record in Scopus

Zhuang et al., 2011

K. Zhuang, M. Izallalen, P. Mouser, H. Richter, C. Risso, R. Mahadevan, D.R. Lovley**Genome-scale dynamic modeling of the competition between *Rhodoferax* and *Geobacter* in anoxic subsurface environments**

ISME J., 5 (2011), pp. 305-316

CrossRefView Record in Scopus